

PNAS



1

2 **Supplementary Information for**

3 **Transport Coefficient Approach for Characterizing Non-equilibrium Dynamics in Soft Matter**

4 **H. He, H. Liang, M. Chu, Z. Jiang, J. J. de Pablo*, M. V. Tirrell*, S. Narayanan*, W. Chen***

5 ***To whom correspondence should be addressed. E-mail: wchen@anl.gov, sureshn@anl.gov, mtirrell@uchicago.edu,**
6 **depablo@uchicago.edu**

7 **This PDF file includes:**

8 Supplementary text

9 Figs. S1 to S13

10 References for SI reference citations

11 Supporting Information Text

12 1. Abbreviation

13 • Mathematical Operation:

- 14 – \mathcal{F} : Fourier Transform
- 15 – \mathbb{E} : Ensemble Average
- 16 – \mathbb{V} : Variance of the quantity as $\mathbb{V}[x] = \mathbb{E}[x^2] - \mathbb{E}[x]^2$
- 17 – Cov: Covariance of two quantities as $\text{Cov}[x, y] = \mathbb{E}[xy] - \mathbb{E}[x]\mathbb{E}[y]$
- 18 – $(f * g)[t]$: Convolution of function $f(t)$ and $g(t)$, equivalent to $\int_{-\infty}^{\infty} f(\tau)g(t - \tau) d\tau$
- 19 – $(f \star g)(\tau)$: Correlation between function $f(t)$ and $g(t)$, equivalent to $\int_{-\infty}^{\infty} f(t)g(t + \tau)dt$.
- 20 – $\vec{u} \otimes \vec{v}$: Outer product of vector \vec{u} and \vec{v}
- 21 – **Re**: taking the real part from the complex composition given as $\mathbf{Re}[e^{iA}] = \mathbf{Re}[i \sin(A) + \cos(A)] = \cos(A)$
- 22 – $\underline{\mathbf{A}}^T$: Transpose of $\underline{\mathbf{A}}$ tensor.

23 • Scattering:

- 24 – $E(\vec{q}, t)$: Scattered electromagnetic wave profile at time t
- 25 – $I(\vec{q}, t)$: Scattered intensity profile at time t
- 26 – b : Scattering contrast of individual particles in the system.
- 27 – $c(\vec{r}, t_1, t_2)$: Correlation function in real space between t_1 and t_2
- 28 – $c_1(\vec{q}, t_1, t_2)$: The first-order two-time correlation function in the reciprocal space between t_1 and t_2 .
- 29 – $c_2(\vec{q}, t_1, t_2)$: The second-order two-time correlation function in the reciprocal space between t_1 and t_2 .
- 30 – $g_1(\vec{q}, \tau)$: The first-order one-time correlation function in the reciprocal space
- 31 – $g_2(\vec{q}, \tau)$: The second-order one-time correlation function in the reciprocal space
- 32 – β : Speckle contrast of the incident beam.
- 33 – $x_n(t)$: The fraction of the individual component n in the system at time t . Follow with the relation $1 = \sum_{n=1}^N x_n(t)$,
34 with N being the total number of components.
- 35 – ϕ_n : The angle between flow velocity and scattering vector \vec{q} for n .
- 36 – f : the normalization factor in a system with multiple compositions.

37 • Probability:

- 38 – $\Delta\vec{r}(t_1, t_2)$: Displacement of a particle between t_1 and t_2 .
- 39 – $\zeta(t)$: The state variable that varies in the random process.
- 40 – $\mathbb{P}(x, t|x_0, v_0)$: The probability density function for position of a particle (x) at time t given the initial conditions
41 $\mathbb{P}(x, v, t = 0) = \delta(x - x_0)\delta(v - v_0)$.
- 42 – $\mathbb{P}(\Delta x, t_1, t_2)$: Transition probability function of a particle making a displacement of Δx as time evolves from t_1 to
43 t_2 .
- 44 – $\mathbb{P}(x_2, t_2|x_1, t_1)$: Joint probability function of $\mathbb{P}(x_1, t_1|x_0, v_0)$ and $\mathbb{P}(x_2, t_2|x_0, v_0)$.
- 45 – J : Transport coefficient defined at Equation S-38.
- 46 – $\mathcal{N}(x; \mu, \sigma^2)$: A normalized Gaussian function with respect to x with a mean of μ and a variance of σ^2 .

47 • Langevin Equation:

- 48 – γ : The friction coefficient or drift that characterizes the effect of friction on the particle's motion.
- 49 – η : A 'truly random' force or noise independent of the particle's state of motion.
- 50 – Γ : The magnitude of the random force depending on collisions between the particles and the solvent, given as
51 $\Gamma = 2m\gamma k_B T$ for one-dimensional system.
- 52 – ω_o : Force constant for the Brownian oscillator, given as $V(x) = \frac{1}{2}m\omega_o^2 x^2$.
- 53 – ω_s : The reduced frequency given as $\omega_s = (\omega_o^2 - \frac{1}{4}\gamma^2)^{\frac{1}{2}}$.

- 54 – γ_s : The reduced drift is given as $\gamma_s = (\gamma^2 - 4\omega_o^2)^{\frac{1}{2}}$.
- 55 – D : The classical diffusion constant in the equilibrium state is defined as $D = \frac{k_B T}{m\gamma}$.
- 56 – D_o : The intrinsic diffusion constant of the system in the equilibrium state.

57 • **Rheology:**

- 58 – γ : Strain in response to the applied deformation.
- 59 – $\dot{\gamma}$: Shear rate in a laminar flow system.
- 60 – σ : Stress applied to the system.
- 61 – \mathcal{J} : Creep compliance, defined as γ/σ .

62 • **Acronym:**

- 63 – XPCS: X-ray Photon Correlation Spectroscopy
- 64 – Rheo-XPCS: combined XPCS and *in situ* Rheology
- 65 – MD: Molecular Dynamics

66 **2. Derivation of the Non-equilibrium model**

67 **A. Correlation Function in X-ray Photon Correlation Spectroscopy (XPCS).** To understand the physical picture of XPCS, we
 68 first start with a system composed of N scattered points. The spatial distribution at time t can be described by the function
 69 denoted as:

$$70 \sum_{n=1}^N \delta(\vec{r} - \vec{r}_n(t)) \quad [S-1]$$

71 In real space, this position function quantifies the relation between the positions of points at different times.

72 The profile of its scattered electromagnetic intensity is derived through a Fourier transform (\mathcal{F}), expressed as:

$$73 \begin{aligned} E(\vec{q}, t) &= \mathcal{F} \left[\sum_{n=1}^N b_n(t) \delta(\vec{r} - \vec{r}_n(t)) \right] = \sum_{n=1}^N b_n(t) e^{i\vec{q} \cdot \vec{r}_n(t)} \\ I(\vec{q}, t) &= |E(\vec{q}, t)|^2 = E(\vec{q}, t) E^*(\vec{q}, t) \\ &= \sum_{n=1}^N \sum_{m=1}^N b_n(t) b_m(t) e^{i\vec{q} \cdot (\vec{r}_n(t) - \vec{r}_m(t))} \end{aligned} \quad [S-2]$$

74 where $b_n(t)$ in the equation S-2 is defined as the unit scattering contrast and \vec{q} is the scattering vector in reciprocal space.

75 The correlation function $c(\vec{r}, t_1, t_2)$ between t_1 and t_2 in real space could be calculated by following:

$$76 c(\vec{r}, t_1, t_2) = \mathbb{E} \left[\sum_{n=1}^N \sum_{m=1}^N \delta(\vec{r} - (\vec{r}_n(t_2) - \vec{r}_m(t_1))) \right] \quad [S-3]$$

77 where $\vec{r}_n(t_2) - \vec{r}_m(t_1)$ is the spatial correlation of any particle n and m between t_1 and t_2 and \mathbb{E} denotes ensemble average .

78 During XPCS measurements, the first order two-time intensity autocorrelation function (c_1) is the temporal correlation of
 79 electromagnetic fields as the average of equation S-3 in the reciprocal space. To match with the physical picture, a Fourier
 80 transform (\mathcal{F}) is applied to the correlation function in real space S-3.

$$81 \mathbb{E} [E(\vec{q}, t_2) E^*(\vec{q}, t_1)] = \mathcal{F} [\mathbb{E} [c(\vec{r}, t_1, t_2)]] = \mathbb{E} \left[\sum_{n=1}^N \sum_{m=1}^N b_n(t_2) b_m(t_1) e^{i\vec{q} \cdot (\vec{r}_n(t_2) - \vec{r}_m(t_1))} \right] \quad [S-4]$$

82 For the random dynamical process in the ensemble, each particle is assumed independent. In equation S-4, the terms where
 83 $n \neq m$ average out to zero (1, at eq. (1.6)). For the $n = m$ terms, the average intensity and correlation of the electromagnetic
 84 field can be expressed as:

$$85 \begin{aligned} \mathbb{E} [I(\vec{q}, t)] &= \mathbb{E} \left[\sum_{n=1}^N b_n(t)^2 e^{i\vec{q} \cdot (\vec{r}_n(t) - \vec{r}_n(t))} \right] = \mathbb{E} \left[\sum_{n=1}^N b_n(t)^2 e^{i\vec{q} \cdot \vec{0}} \right] = \mathbb{E} \left[\sum_{n=1}^N b_n(t)^2 \right] \\ \mathbb{E} [E(\vec{q}, t_2) E^*(\vec{q}, t_1)] &= \mathbb{E} \left[\sum_{n=1}^N b_n(t_1) b_n(t_2) e^{i\vec{q} \cdot (\vec{r}_n(t_2) - \vec{r}_n(t_1))} \right] = \mathbb{E} \left[\sum_{n=1}^N b_n(t_1) b_n(t_2) e^{i\vec{q} \cdot \Delta \vec{r}(t_1, t_2)} \right] \end{aligned} \quad [S-5]$$

86 where $\Delta\vec{r}(t_1, t_2)$ is defined as the displacement of one particle between t_1 and t_2 , given by $\Delta\vec{r}(t_1, t_2) = \vec{r}_n(t_2) - \vec{r}_n(t_1)$.

87 In the case where the system is composed of monodisperse spheres, with all particles having the same contrast and lacking
88 any time and direction dependence as $b_n(t) = b_n$, this common factor can be extracted from the average.

$$\begin{aligned} \mathbb{E}[I(\vec{q}, t)] &= \mathbb{E}\left[\sum_{n=1}^N b_n^2\right] = Nb_n^2 \\ \mathbb{E}[E(\vec{q}, t_2)E^*(\vec{q}, t_1)] &= \mathbb{E}\left[\sum_{n=1}^N b_n^2 e^{i\vec{q}\cdot(\vec{r}_n(t_2) - \vec{r}_n(t_1))}\right] = Nb_n^2 \mathbb{E}\left[e^{i\vec{q}\cdot\Delta\vec{r}(t_1, t_2)}\right] \end{aligned} \quad \text{[S-6]}$$

90 Consequently, $c_1(\vec{q}, t_1, t_2)$ is obtained by normalizing the correlation function by $|b_n|^2$. (2, at eq. (3.4.14))

$$\begin{aligned} c_1(\vec{q}, t_1, t_2) &= \frac{\mathbb{E}[E(\vec{q}, t_2)E^*(\vec{q}, t_1)]}{\left[\mathbb{E}[|E(\vec{q}, t_1)|^2] \mathbb{E}[|E(\vec{q}, t_2)|^2]\right]^{\frac{1}{2}}} = \frac{\mathbb{E}[E(\vec{q}, t_2)E^*(\vec{q}, t_1)]}{\left[\mathbb{E}[I(\vec{q}, t_1)] \mathbb{E}[I(\vec{q}, t_2)]\right]^{\frac{1}{2}}} \\ &= \frac{Nb_n^2 \mathbb{E}\left[e^{i\vec{q}\cdot\Delta\vec{r}(t_1, t_2)}\right]}{Nb_n^2} = \mathbb{E}\left[e^{i\vec{q}\cdot\Delta\vec{r}(t_1, t_2)}\right] \end{aligned} \quad \text{[S-7]}$$

92 To establish a correlation between $c_1(\vec{q}, t_1, t_2)$ and the dynamics of particles, we consider a system where the particle
93 distribution at any time t after $t_0 = 0$ follows a probability density function described by $\mathbb{P}(\vec{r}, t|t_0 = 0)$. We then define
94 $\mathbb{P}(\Delta\vec{r}, t_1, t_2)$ as the transition probability of a particle with displacement ($\Delta\vec{r} = \vec{r}_2 - \vec{r}_1$) between time t_1 and time t_2 . Then
95 the relation between the probability distribution function at t_1 and t_2 can be connected with the transition probability as
96 follows,

$$\begin{aligned} \mathbb{P}(\vec{r}_2, t_2|t_0 = 0) &= \int_{-\infty}^{\infty} \mathbb{P}(\vec{r}_1, t_1|t_0 = 0) \mathbb{P}(\Delta\vec{r}, t_1, t_2) d\vec{r}_1 \\ &= \int_{-\infty}^{\infty} \mathbb{P}(\vec{r}_1, t_1|t_0 = 0) \mathbb{P}(\vec{r}_2, t_2|\vec{r}_1, t_1) d\vec{r}_1 \end{aligned} \quad \text{[S-8]}$$

98 In a Markov chain, where its behavior depends only on its current state but not on its past, the variable t_1 is excluded from
99 the computation process in Equation (S-8). If $\mathbb{P}(\Delta\vec{r}, t_1, t_2)$ is known, the c_1 in equation S-7 can be expressed equivalently as
100 follows:

$$c_1(\vec{q}, t_1, t_2) = \mathbb{E}\left[e^{i\vec{q}\cdot\Delta\vec{r}}\right] = \int_{-\infty}^{\infty} \mathbb{P}(\Delta\vec{r}, t_1, t_2) e^{i\vec{q}\cdot\Delta\vec{r}} d\Delta\vec{r} \quad \text{[S-9]}$$

102 By converting the $c_1(\vec{q}, t_1, t_2)$ to the second order correlation function $c_2(\vec{q}, t_1, t_2)$ with Siegert relation, we can obtain the
103 experiment measurement of the XPCS.

$$c_2(\vec{q}, t_1, t_2) = 1 + \beta |c_1(\vec{q}, t_1, t_2)|^2 = \frac{\mathbb{E}[I(\vec{q}, t_1)I(\vec{q}, t_2)]}{\mathbb{E}[I(\vec{q}, t_1)] \mathbb{E}[I(\vec{q}, t_2)]} \quad \text{[S-10]}$$

105 where β is the speckle contrast range from 0-1 depending on the coherence of the incident beam and $I(\vec{q}, t)$ is the time-resolved
106 intensity profile at specific \vec{q} and time t .

107 **B. Generalized Model: Markov Chain with Gaussian Random Walk.** To gain a preliminary understanding of the dynamics of a
108 complicated non-equilibrium system, it is assumed that the particles undergo a Gaussian random walk in 1-dimension. The
109 step size for each walk varies according to a normal distribution. This dynamic behavior is described as a Markov process,
110 where the evolution at a certain time t for $t > t_0$ does not depend on any of the previous states the system had been in before
111 t . Instead, it relies only on the state of the system at time t . This process represents the simplest form of a system without
112 memory, where the present distribution defines the future distribution.

113 In this Markov process, the n -time probability distribution for the process, denoted as $\mathbb{P}(\zeta_n, t_n)$, is defined as (3, at eq.
114 (5.3)).

$$\begin{aligned} n\text{-component general process : } \zeta(t) &= (\zeta_0(t), \dots, \zeta_n(t)) \\ \mathbb{P}(\zeta_n, t_n) &= \mathbb{P}(\zeta_n, t_n|\zeta_{n-1}, t_{n-1}) \dots \mathbb{P}(\zeta_1, t_1|\zeta_0, t_0) \mathbb{P}(\zeta_0, t_0) \\ \mathbb{P}(\zeta_n, t_n) &= \int_{-\infty}^{\infty} \dots \int_{-\infty}^{\infty} \left[\prod_{t=t_0}^{t_n} \mathbb{P}(x_t, t|x_{t-1}, t_{t-1}) \right] \mathbb{P}(\zeta_0, t_0) dx_{t_0} \dots dx_{t_n} \end{aligned} \quad \text{[S-11]}$$

116 where $\zeta(t)$ is the state variable that varies in the random process and $\mathbb{P}(\zeta_n, t_n|\zeta_{n-1}, t_{n-1})$ is defined as the transition
117 probability of states from time t_{n-1} to t_n .

118 In the Gaussian random walk model in 1-dimension, the state variable $\zeta(t)$ represents the position (x) of the particle, which
 119 varies during the random process. The transition probability of states from time t_{n-1} to t_n , is denoted as

$$\begin{aligned}
 \mathbb{P}(x_n, t_n | x_{n-1}, t_{n-1}) &= \frac{1}{\sqrt{2\pi J(t_n)\Delta t}} e^{-\frac{\Delta x^2}{2J(t_n)\Delta t}} = \frac{1}{\sqrt{2\pi J(t_n)\Delta t}} e^{-\frac{(x_n - x_{n-1})^2}{2J(t_n)\Delta t}} \\
 &\triangleq \mathcal{N}(x_n - x_{n-1}; \mu = 0, \sigma^2 = J(t_n)\Delta t) \\
 &\triangleq \mathcal{N}(x_n; \mu = x_{n-1}, \sigma^2 = J(t_n)\Delta t) \\
 &\triangleq \mathcal{N}(x_{n-1}; \mu = x_n, \sigma^2 = J(t_n)\Delta t)
 \end{aligned}
 \tag{S-12}$$

121 This transition probability is a key element in the Gaussian random walk model, where each step follows a Gaussian
 122 distribution and the state variable evolves based on these transitions. Δx is the step the particles take from t_{n-1} to t_n , defined
 123 as $\Delta x = x_n - x_{n-1}$, and Δt is the time interval between adjacent steps t_n and t_{n-1} , given by $\Delta t = t_n - t_{n-1}$. $J(t_n)\Delta t$ is the
 124 standard deviation of the step size. $J(t_n)$ is the transport coefficient corresponding to the transition step in $t_{n-1} \rightarrow t_n$. We
 125 will define transport coefficient ($J(t)$) physically and mathematically at equation S-38 later.

126 To obtain the correlation function $c_1(\vec{q}, t_1, t_2)$ for any two states at time t_2 and t_1 with an arbitrary number of steps between
 127 them, we need to calculate the transition probability $\mathbb{P}(x_2, t_2 | x_1, t_1)$. According to the Chapman-Kolmogorov Equation,
 128 $\mathbb{P}(x_2, t_2 | x_1, t_1)$ can be expressed as the product of the probabilities of propagating from t_1 to all intermediate values $t - t'$ for
 129 $t_1 < t' < t_2$, and subsequently to t_2 , summed over all possible values of the intermediate state. The expression is given as:

$$\mathbb{P}(x_2, t_2 | x_1, t_1) = \int_{-\infty}^{\infty} \cdots \int_{-\infty}^{\infty} \left[\prod_{t=t_1}^{t_2-\Delta t} \mathbb{P}(x_{t+\Delta t}, t + \Delta t | x_t, t) \right] \mathbb{P}(x_{t_1}, t_1 | x_1, t_1), dx_{t_1} \cdots dx_{t_2-\Delta t}
 \tag{S-13}$$

131 where Δt is the time interval between consecutive states, and the product represents the joint probabilities of propagating
 132 from t to $t + \Delta t$ for each intermediate time interval. This integral sums up all possible intermediate states between t_1 and t_2 ,
 133 and allows us to calculate the transition probability from an initial state x_1 at time t_1 to a final state x_2 at t_2 considering all
 134 possible paths and intermediate states.

135 In the transition probability for any two nearby steps $\mathbb{P}(x_c, t_c | x_a, t_a)$ at $t_a \rightarrow t_b$ and $t_b \rightarrow t_c$, according to equation S-12
 136 and S-13, is

$$\begin{aligned}
 \mathbb{P}(x_c, t_c | x_a, t_a) &= \int_{-\infty}^{\infty} \mathbb{P}(x_c, t_c | x_b, t_b) \mathbb{P}(x_b, t_b | x_a, t_a) dx_b \\
 &= \int_{-\infty}^{\infty} \mathcal{N}(x_c - x_b; \mu = 0, \sigma^2 = J(t_c)\Delta t) \mathcal{N}(x_b - x_a; \mu = 0, \sigma^2 = J(t_b)\Delta t) dx_b \\
 &= \int_{-\infty}^{\infty} \mathcal{N}(x_c - x_b; \mu = 0, \sigma^2 = J(t_c)\Delta t) \mathcal{N}(x_b; \mu = x_a, \sigma^2 = J(t_b)\Delta t) dx_b
 \end{aligned}
 \tag{S-14}$$

138 The equation S-14 is a convolution operation of Gaussian function as $\tau = x_b$ with the property of resulting in a new Gaussian
 139 function with a mean of $\mu = \mu_f + \mu_g$ and variance of $\sigma^2 = \sigma_f^2 + \sigma_g^2$ as follow:

$$\begin{aligned}
 (f * g)[t] &= \int_{-\infty}^{\infty} f(\tau)g(t - \tau) d\tau \\
 (\mathcal{N}(\tau; \mu_f, \sigma_f^2) * \mathcal{N}(t - \tau; \mu_g, \sigma_g^2))[t] &= \mathcal{N}(t; \mu_f + \mu_g, \sigma_f^2 + \sigma_g^2)
 \end{aligned}
 \tag{S-15}$$

141 Substituting the relation at S-15 to equation S-14, $\mathbb{P}(x_c, t_c | x_a, t_a)$ is obtained as follow:

$$\begin{aligned}
 \mathbb{P}(x_c, t_c | x_a, t_a) &= \mathcal{N}(x_c - x_b; \mu = 0, \sigma^2 = J(t_c)\Delta t) * \mathcal{N}(x_b; \mu = x_a, \sigma^2 = J(t_b)\Delta t) [x_c] \\
 &= \mathcal{N}(x_c; \mu = x_a, \sigma^2 = J(t_c)\Delta t + J(t_b)\Delta t) \\
 &= \mathcal{N}(x_c - x_a; \mu = 0, \sigma^2 = (J(t_c) + J(t_b))\Delta t)
 \end{aligned}
 \tag{S-16}$$

143 Expanding the result from S-16 to S-13, we can obtain $\mathbb{P}(x_2, t_2 | x_1, t_1)$ as follow:

$$\mathbb{P}(x_2, t_2 | x_1, t_1) = \mathcal{N}\left(x_2 - x_1; \mu = 0, \sigma^2 = \Delta t \sum_{t=t_1}^{t_2} J(t)\right)
 \tag{S-17}$$

145 Adapting an assumption that step difference is infinitesimal that there is infinity t' between t_2 and t_1 , the summation
 146 $\Delta t \sum_{t'=t_1}^{t_2} J(t')$ can be expressed as an integration of a continuous function $J(t)$ as:

$$\Delta t \sum_{t=t_1}^{t_2} J(t) = \int_{t_1}^{t_2} J(t) dt \quad [S-18]$$

$$\mathbb{P}(x_2, t_2 | x_1, t_1) = \mathcal{N} \left(x_2 - x_1; \mu = 0, \sigma^2 = \int_{t_1}^{t_2} J(t) dt \right)$$

148 where $J(t)$ is a continuous function of the change in the distribution standard deviation in $\mathbb{P}(x, t)$ as time evolves.

149 Considering $x_2 - x_1 = \Delta x$, we in fact obtain the $\mathbb{P}(\Delta x, t_1, t_2)$. The $c_1(q, t_1, t_2)$ is calculated according to the equation S-4
 150 as:

$$\begin{aligned} c_1(q, t_1, t_2) &= \int_{-\infty}^{\infty} \mathbb{P}(\Delta x, t_1, t_2) e^{iq\Delta x} d\Delta x \\ &= \int_{-\infty}^{\infty} \mathcal{N} \left(\Delta x; \mu = 0, \sigma^2 = \int_{t_1}^{t_2} J(t) dt \right) e^{iq\Delta x} d\Delta x \\ &= \frac{1}{\sqrt{2\pi \int_{t_1}^{t_2} J(t) dt}} \int_{-\infty}^{\infty} e^{-\frac{\Delta x^2}{2 \int_{t_1}^{t_2} J(t) dt} + iq\Delta x} d\Delta x \\ &= e^{-\frac{1}{2}q^2 \int_{t_1}^{t_2} J(t) dt} \end{aligned} \quad [S-19]$$

152 Considering the Siegert relation, the $c_2(q, t_1, t_2)$ obtained from XPCS measurement for the Gaussian random walk process is
 153 defined as:

$$c_2(q, t_1, t_2) = 1 + \beta |c_1(q, t_1, t_2)|^2 = \beta e^{-q^2 \int_{t_1}^{t_2} J(t) dt} + 1 \quad [S-20]$$

155 This equation describes the $c_2(\vec{q}, t_1, t_2)$ of a system constituted of particles undergoing random Gaussian walk.

156 **C. Derivation of $c_1(q, t_1, t_2)$ from Langevin Equation.** Begin with Newton's equation of motion for particles in 1-dimension:

$$m\dot{v} = F(t) = F_{in}(t) + F_{ex}(t) \quad [S-21]$$

158 where $F(t)$ is the total force on the particles includes internal F_{in} and external F_{ex} force. When the internal force includes a
 159 random force $\eta(t)$ and a systematic force $F_{sys}(x, v, t)$ depends on the state of particle motion,

$$F_{in}(t) = F_{sys}(x, v) + \eta(t) \quad [S-22]$$

161 In a simple system, F_{sys} only contains a drift force $m\gamma v(t)$ act in the opposite direction to its motion to prevent large velocity
 162 fluctuations from building up. Therefore, the expression of F_{in} is

$$F_{in} = -m\gamma v(t) + \eta(t) \quad [S-23]$$

164 We then have the Langevin Equation as:

$$m\dot{v} = -m\gamma v(t) + \eta(t) + F_{ex}(t) \quad [S-24]$$

166 In this equation, $v(t)$ represents the velocity of the particle, and m denotes its mass. The parameter γ is a positive constant
 167 referred to as the friction coefficient or drift, which characterizes the effect of friction on the particle's motion. The term $\eta(t)$
 168 denotes a 'truly random' force or noise independent of the state of motion of the particle. It has a 1st moment of zero and
 169 2nd moment proportional to thermal fluctuations with a factor of Γ , which, according to fluctuation-dissipation theorem, is
 170 $\Gamma = 2m\gamma k_B T$,

$$\begin{aligned} \mathbb{E}[\eta(t)] &= 0 \\ \mathbb{E}[\eta(t)\eta(t')] &= \Gamma\delta(t-t') \end{aligned} \quad [S-25]$$

172 Finally, F_{ex} represents the result of all external applied forces acting on individual particles, which we consider identical
 173 throughout the paper.

174 From solving the Langevin Equation, the velocity of individual particle $v(t)$, mean velocity $\mathbb{E}[v(t)]$ and mean position
 175 $\mathbb{E}[x(t)]$ of the ensemble can be expressed as: (3, at eq. (2.19, 3.3 and 11.14))

$$\begin{aligned}
 v(t) &= v_o e^{-\gamma t} + \frac{1}{m} \int_0^t dt' e^{-\gamma(t-t')} [\eta(t') + F_{ex}(t')] \\
 \mathbb{E}[v(t)] &= v_o e^{-\gamma t} + \mathbb{E} \left[\frac{1}{m} \int_0^t dt' e^{-\gamma(t-t')} [\eta(t') + F_{ex}(t')] \right] \\
 &= v_o e^{-\gamma t} + \frac{1}{m} \int_0^t dt' e^{-\gamma(t-t')} F_{ex}(t') \\
 \mathbb{E}[x(t)] &= x_0 + \frac{v_o}{\gamma} (1 - e^{-\gamma t}) + \frac{1}{m} \int_0^t dt' \int_0^{t'} dt'' e^{-\gamma(t'-t'')} F_{ex}(t'')
 \end{aligned} \tag{S-26}$$

177 From the velocity $v(t)$, the temporal correlation of velocity $\mathbb{E}[v(t)v(t')]$, the mean square average of the position $\mathbb{E}[x(t)^2]$,
 178 and the variance of the position distribution $\mathbb{V}[x(t)]$ exhibit following relations: (3, at eq. (15.2)) (4, at eq. (2.186))

$$\begin{aligned}
 \mathbb{E}[x(t)^2] &= x_0^2 + \int_0^t dt_1 \int_0^t dt_2 \mathbb{E}[v(t_1)v(t_2)] \\
 \mathbb{V}[x(t)] &= \mathbb{E}[x(t)^2] - \mathbb{E}[x(t)]^2
 \end{aligned} \tag{S-27}$$

180 For any stochastic process exhibiting the Markov Chain characteristic, and when all particles in the system have the same
 181 initial conditions of position $x(t=0) = x_0$ and velocity $v(t=0) = v_o$, as:

$$\mathbb{P}(x, v, t=0) = \delta(x - x_0) \delta(v - v_o) \tag{S-28}$$

183 the probability distribution function at any given time t can be represented by a Gaussian function. This Gaussian distribution
 184 depends on the known mean $\mathbb{E}[x(t)]$ and variance $\mathbb{V}[x(t)]$, for that specific moment.

$$\begin{aligned}
 \mathbb{P}(x, t|x_0, t=0) &= \int_{-\infty}^{\infty} \mathbb{P}(x, v, t|x_0, v_o, t=0) dv \\
 &= \frac{1}{\sqrt{2\pi\mathbb{V}[x(t)]}} \exp\left(-\frac{[x - \mathbb{E}[x(t)]]^2}{2\mathbb{V}[x(t)]}\right) \\
 &= \mathcal{N}(x; \mu = \mathbb{E}[x(t)], \sigma^2 = \mathbb{V}[x(t)])
 \end{aligned} \tag{S-29}$$

186 According to the Equation (S-18), $\mathbb{P}(x, t|x_0, v_o)$ at any time t can be rewritten as:

$$\begin{aligned}
 \mathbb{E}[x(t)] &= x_0 + \int_0^t \mathbb{E}[v(t)] dt \\
 \mathbb{V}[x(t)] &= \int_0^t J(t) dt \\
 \mathbb{P}(x, t|x_0, v_o) &= \mathcal{N}\left(x; \mu = x_0 + \int_0^t \mathbb{E}[v(t)] dt, \sigma^2 = \int_0^t J(t) dt\right)
 \end{aligned} \tag{S-30}$$

188 with the initial conditions according to Equation (S-28),

$$\begin{aligned}
 \mathbb{E}[x(0)] &= x_0 \\
 \mathbb{V}[x(0)] &= 0
 \end{aligned} \tag{S-31}$$

190 To obtain the transition probability $\mathbb{P}(\Delta x, t_2, t_1)$ between t_1 and t_2 , we apply the Fourier transform to both sides of
 191 Equation (S-8),

$$\mathcal{F}[\mathbb{P}(x_2, t_2|x_0, t=0)] = \mathcal{F}[\mathbb{P}(x_1, t_1|x_0, t=0)] \mathcal{F}[\mathbb{P}(\Delta x, t_2, t_1)] \tag{S-32}$$

193 so

$$\mathbb{P}(\Delta x, t_2, t_1) = \mathcal{F}^{-1} \left[\frac{\mathcal{F}[\mathbb{P}(x_2, t_2|x_0, t=0)]}{\mathcal{F}[\mathbb{P}(x_1, t_1|x_0, t=0)]} \right] \tag{S-33}$$

195 Considering the special property of Gaussian-like function in Fourier transform,

$$\mathcal{F}[\mathcal{N}(x; \mu, \sigma^2)] = e^{-\frac{\sigma^2}{2} q^2 - i\mu q} \tag{S-34}$$

197 $\mathbb{P}(\Delta x, t_2, t_1)$ is obtained as

$$\begin{aligned}
\mathbb{P}(\Delta x, t_2, t_1) &= \mathcal{F}^{-1} \left[\frac{\exp\left(-\frac{\mathbb{V}[x(t_2)]}{2} q^2 - i \mathbb{E}[x(t_2)] q\right)}{\exp\left(-\frac{\mathbb{V}[x(t_1)]}{2} q^2 - i \mathbb{E}[x(t_1)] q\right)} \right] \\
&= \mathcal{F}^{-1} \left[\exp\left(-\frac{(\mathbb{V}[x(t_2)] - \mathbb{V}[x(t_1)])}{2} q^2 - i (\mathbb{E}[x(t_2)] - \mathbb{E}[x(t_1)]) q\right) \right] \\
&= \mathcal{N}(\Delta x; \mu = \mathbb{E}[x(t_2)] - \mathbb{E}[x(t_1)], \sigma^2 = \mathbb{V}[x(t_2)] - \mathbb{V}[x(t_1)])
\end{aligned} \tag{S-35}$$

199 The transition probability between two Gaussian-like probability functions preserves the Gaussian shape, and the resulting
200 Gaussian function will have its mean shifted by the difference between the means of the original Gaussian functions ($\mathbb{E}[x(t_2)] -$
201 $\mathbb{E}[x(t_1)]$) and its variance scaled by the difference between the variances of the original Gaussian functions ($\mathbb{V}[x(t_2)] - \mathbb{V}[x(t_1)]$)
202 based on the specific values of the original Gaussian functions.

203 We then define the change in the mean position of a particle as time evolves from t_1 to t_2 , $\mathbb{E}[x(t_2)] - \mathbb{E}[x(t_1)]$, as the
204 integration of mean velocity from t_1 to t_2 ; the change in the variance of the position distribution $\mathbb{V}[x(t_2)] - \mathbb{V}[x(t_1)]$, as the
205 integration of dynamical transport coefficient $J(t)$ from t_1 to t_2 :

$$\mathbb{P}(\Delta x, t_1, t_2) = \mathcal{N}\left(\Delta x; \mu = \int_{t_1}^{t_2} \mathbb{E}[v(t)] dt, \sigma^2 = \int_{t_1}^{t_2} J(t) dt\right) \tag{S-36}$$

207 so that relation Equation (S-8) is clearly satisfied as follow:

$$\begin{aligned}
\mathbb{P}(x_2, t_2 | x_0, t = 0) &= \int_{-\infty}^{\infty} \mathbb{P}(x_1, t_1 | x_0, t = 0) \mathbb{P}(\Delta x, t_1, t_2) dx_1 \\
&= \left(\mathcal{N}\left(x_1; \mu = x_0 + \int_0^{t_1} \mathbb{E}[v(t)] dt, \sigma^2 = \int_0^{t_1} J(t) dt\right) * \mathcal{N}\left(\Delta x; \mu = \int_{t_1}^{t_2} \mathbb{E}[v(t)] dt, \sigma^2 = \int_{t_1}^{t_2} J(t) dt\right) \right) [x_1] \\
&= \mathcal{N}\left(x_2; \mu = x_0 + \int_0^{t_2} \mathbb{E}[v(t)] dt, \sigma^2 = \int_0^{t_2} J(t) dt\right)
\end{aligned} \tag{S-37}$$

208 which is consistent with the definition in Equation (S-30).

210 In Equation (S-36), we define the change in the mean position of a particle as time evolves from t_1 to t_2 , $\mathbb{E}[x(t_2)] - \mathbb{E}[x(t_1)]$,
211 as the integration of mean velocity from t_1 to t_2 ; the change in variance of the position distribution $\mathbb{V}[x(t_2)] - \mathbb{V}[x(t_1)]$, as the
212 integration of the dynamical transport coefficient $J(t)$ from t_1 to t_2 :

213 The mathematical and physical definition of the transport coefficient $J(t)$ is shown as:

$$\begin{aligned}
J(t) &= \frac{d}{dt}(\mathbb{V}[x(t)]) \\
&= 2(\mathbb{E}[x(t)v(t)] - \mathbb{E}[x(t)]\mathbb{E}[v(t)]) = 2\text{Cov}[x(t), v(t)] \\
&= 2\left(\mathbb{E}\left[\int_0^t v(t')v(t) dt'\right] - \mathbb{E}\left[\int_0^t v(t') dt'\right]\mathbb{E}[v(t)]\right) \\
&= 2\left(\int_0^t \mathbb{E}[v(t')v(t)] dt' - \int_0^t \mathbb{E}[v(t')]\mathbb{E}[v(t)] dt'\right) \\
&= 2\int_0^t \text{Cov}[v(t), v(t')] dt'
\end{aligned} \tag{S-38}$$

215 where $\text{Cov}[x(t), v(t)]$ is the covariance of $x(t)$ and $v(t)$ and $\int_0^t \text{Cov}[v(t), v(t')] dt'$ is a generalized form of Green-Kubo formula
216 (3, at eq. (15.3)).

217 From eq. (S-36), we have following expression:

$$\mathbb{P}(\Delta x, t_1, t_2) = \frac{1}{\sqrt{2\pi \int_{t_1}^{t_2} J(t) dt}} \exp\left(-\frac{\left[\Delta x - \int_{t_1}^{t_2} \mathbb{E}[v(t)] dt\right]^2}{2 \int_{t_1}^{t_2} J(t) dt}\right) \tag{S-39}$$

At the end, the two-time correlation function $c_1(q, t_1, t_2)$, at specific scattering vector q , can be expressed as:

$$\begin{aligned}
c_1(q, t_1, t_2) &= \int_{-\infty}^{\infty} \mathbb{P}(\Delta x, t_1, t_2) e^{iq\Delta x} d\Delta x \\
&= \frac{1}{\sqrt{2\pi \int_{t_1}^{t_2} J(t) dt}} \int_{-\infty}^{\infty} \exp\left(-\frac{\left[\Delta x - \int_{t_1}^{t_2} \mathbb{E}[v(t)] dt\right]^2}{2 \int_{t_1}^{t_2} J(t) dt} + iq\Delta x\right) d\Delta x \\
&= e^{-\frac{1}{2}q^2 \int_{t_1}^{t_2} J(t) dt} e^{iq \int_{t_1}^{t_2} \mathbb{E}[v(t)] dt}
\end{aligned} \tag{S-40}$$

Compared to Equation (S-35), Equation (S-40) is equivalent to the Fourier transform of the transition probability. In other words, the correlation function measured in XPCS is the ratio between the Fourier transform of the probability function of a particle at t_1 and t_2 .

$$c_1(q, t_1, t_2) = \mathcal{F}[\mathbb{P}(\Delta x, t_1, t_2)] = \frac{\mathcal{F}[\mathbb{P}(x_2, t_2|x_0, t=0)]}{\mathcal{F}[\mathbb{P}(x_1, t_1|x_0, t=0)]} \tag{S-41}$$

According to eq. (S-40), the $c_1(q, t_1, t_2)$ could be factorized into two terms:

$$c_1(q, t_1, t_2) = c_{1,in}(q, t_1, t_2) c_{1,ex}(q, t_1, t_2) \tag{S-42}$$

where $c_{1,in}(q, t_1, t_2)$ is the correlation function attributed to internal forces, including the systematic dynamics as well as the thermal fluctuations experienced by particles, defined as:

$$c_{1,in}(q, t_1, t_2) = e^{-\frac{1}{2}q^2 \int_{t_1}^{t_2} J(t) dt} \tag{S-43}$$

and $c_{1,ex}(q, t_1, t_2)$ is the correlation function attributed to external drives defined as:

$$c_{1,ex}(q, t_1, t_2) = e^{iq \int_{t_1}^{t_2} \mathbb{E}[v(t)] dt} \tag{S-44}$$

In summary, the $c_1(q, t_1, t_2)$ is obtained by following steps:

1. Formalize Langevin equation based force profile of individual particles
2. Calculate $\mathbb{E}[v(t)]$ and $J(t)$ from Langevin equation.
3. Obtain $c_1(q, t_1, t_2)$ by substituting $\mathbb{E}[v(t)]$ and $J(t)$ into equation S-40

Equation S-40 is the $c_1(q, t_1, t_2)$ for the model of particles with Langevin Dynamics in 1-dimension as a fluid transports with mean velocity ($\mathbb{E}[v(t)]$) due to the bulk movement and transport coefficient $J(t)$ due to molecular random motion.

D. $c_1(\vec{q}, t_1, t_2)$ in 3-Dimensional Space. To extend the analysis to 3-dimension and derive $c_1(\vec{q}, t_1, t_2)$, we start from Langevin equation in 3 dimensions: (3, at eq. (4.9))

$$m\vec{v} = -m\gamma\vec{v} + \eta(t) + \vec{F}_{ex} \tag{S-45}$$

where \vec{v} , $\vec{\eta}$ and \vec{F}_{ex} are the vectors consist all Cartesian components. It is noticed that $\vec{\eta}(t)$ is an independent Gaussian white noise. The mean and autocorrelation of the noise are given by the following straightforward generalizations according to S-25:

$$\begin{aligned}
\mathbb{E}[\vec{\eta}(t)] &= \vec{0} \\
\mathbb{E}[\vec{\eta}(t) \otimes \vec{\eta}(t')]_{ij} &= \Gamma_{ij} \delta(t - t')
\end{aligned} \tag{S-46}$$

where the Cartesian indices i, j run over the values (x, y, z) and Γ_{ij} is the noise strength correlated to direction i, j .

In summary, for the case in the Ornstein-Uhlenbeck process where noises in each dimension are uncorrelated, the partial differential equation can be separated and solved independently as one in 1-dimension.

As the first step of solving $c_1(\vec{q}, t_1, t_2)$ in 3D, the velocity of individual particle $\vec{v}(t)$, mean velocity $\mathbb{E}[\vec{v}(t)]$, and mean position $\mathbb{E}[\vec{r}(t)]$ of the ensemble are solved as:

$$\begin{aligned}
\vec{v}(t) &= \vec{v}_o e^{-\gamma t} + \frac{1}{m} \int_0^t dt' e^{-\gamma(t-t')} [\vec{\eta}(t') + \vec{F}_{ex}(t')] \\
\mathbb{E}[\vec{v}(t)] &= \vec{v}_o e^{-\gamma t} + \frac{1}{m} \int_0^t dt' e^{-\gamma(t-t')} \vec{F}_{ex}(t') \\
\mathbb{E}[\vec{r}(t)] &= \vec{r}_o + \frac{\vec{v}_o}{\gamma} (1 - e^{-\gamma t}) + \frac{1}{m} \int_0^t dt' \int_0^{t'} dt'' e^{-\gamma(t'-t'')} \vec{F}_{ex}(t'')
\end{aligned} \tag{S-47}$$

250 In Ornstein–Uhlenbeck process without external forces, $F_{ex} = 0$, the mean of position at each axis, $\mathbb{E}[\vec{r}(t)]_i$, and velocity
 251 correlation function $\mathbb{E}[v_i(t)v_j(t')]$ can be written as:

$$\begin{aligned} \mathbb{E}[\vec{r}(t)]_i &= r_{o,i} + \frac{v_{o,i}}{\gamma}(1 - e^{-\gamma t}) \\ \mathbb{E}[\vec{v}(t) \otimes \vec{v}(t')]_{ij} &= v_{o,i}v_{o,j}e^{-\gamma(t+t')} + \end{aligned} \quad [S-48]$$

$$\frac{1}{m^2} \int_0^t dt_1 \int_0^{t'} dt_2 e^{-\gamma(t-t_1)-\gamma(t'-t_2)} \mathbb{E}[\eta_i(t_1)\eta_j(t_2)]$$

253 The outer product of mean of velocity $\mathbb{E}[\vec{v}(t)] \otimes \mathbb{E}[\vec{v}(t')]$ can be written as:

$$\mathbb{E}[\vec{v}(t)] \otimes \mathbb{E}[\vec{v}(t')]_{ij} = v_{o,i}v_{o,j}e^{-\gamma(t+t')} \quad [S-49]$$

255 The cross-covariance matrix of velocity at t and t' is calculated as:

$$\begin{aligned} \text{Cov}[\vec{v}(t), \vec{v}(t')]_{ij} &= \mathbb{E}[\vec{v}(t) \otimes \vec{v}(t')]_{ij} - [\mathbb{E}[\vec{v}(t)] \otimes \mathbb{E}[\vec{v}(t')]]_{ij} \\ &= \frac{1}{m^2} \int_0^t dt_1 \int_0^{t'} dt_2 e^{-\gamma(t-t_1)-\gamma(t'-t_2)} \mathbb{E}[\eta_i(t_1)\eta_j(t_2)] \\ &= \frac{\Gamma_{ij}}{m^2} \int_0^t dt_1 \int_0^{t'} dt_2 e^{-\gamma(t-t_1)-\gamma(t'-t_2)} \delta(t_1 - t_2) \\ &= \frac{\Gamma_{ij}}{2m^2\gamma} (e^{-\gamma|t-t'|} - e^{-\gamma(t+t')}) \end{aligned} \quad [S-50]$$

257 The element $J_{ij}(t)$ in transport coefficient tensor \underline{J} is calculated as:

$$\begin{aligned} J_{ij}(t) &= 2 \int_0^t \text{Cov}[\vec{v}(t), \vec{v}(t')]_{ij} dt' \\ &= \frac{\Gamma_{ij}}{m^2\gamma} \int_0^t (e^{-\gamma|t-t'|} - e^{-\gamma(t+t')}) dt' \\ &= \frac{\Gamma_{ij}}{m^2\gamma^2} (1 - 2e^{-\gamma t} + e^{-2\gamma t}) \end{aligned} \quad [S-51]$$

259 Then, the covariance matrix with elements of $\mathbb{V}[\vec{r}(t)]_{ij}$ can be calculated from integrating $\mathbb{V}[\vec{v}(t) \otimes \vec{v}(t')]_{ij}$:

$$\begin{aligned} \mathbb{V}[\vec{r}(t)]_{ij} &= \int_0^t dt_1 \int_0^t dt_2 \text{Cov}[\vec{v}(t_1), \vec{v}(t_2)]_{ij} \\ &= \frac{\Gamma_{ij}}{2m^2\gamma^3} (2\gamma t - 3 + 4e^{-\gamma t} - e^{-2\gamma t}) \\ \underline{\mathbb{V}}[\vec{r}(t)] &= \frac{1}{2m^2\gamma^3} (2\gamma t - 3 + 4e^{-\gamma t} - e^{-2\gamma t}) (\underline{\Gamma}_{i=j} + \underline{\Gamma}_{i \neq j}) \end{aligned} \quad [S-52]$$

$$\underline{\Gamma}_{i=j} = \begin{bmatrix} \Gamma_{xx} & 0 & 0 \\ 0 & \Gamma_{yy} & 0 \\ 0 & 0 & \Gamma_{zz} \end{bmatrix}, \underline{\Gamma}_{i \neq j} = \begin{bmatrix} 0 & \Gamma_{xy} & \Gamma_{xz} \\ \Gamma_{yx} & 0 & \Gamma_{yz} \\ \Gamma_{zx} & \Gamma_{zy} & 0 \end{bmatrix}$$

261 where $(\underline{\Gamma}_{i=j})$ is the variances of the individual dimension and $\underline{\Gamma}_{i \neq j}$ is the covariances across different dimensions.

262 If we assume the noise strength Γ in different directions are truly randomized and uncorrelated, the autocorrelation of noise
 263 $\mathbb{E}[\vec{\eta}(t) \otimes \vec{\eta}(t')]_{ij}$ can be written as: (3, at eq. (4.11))

$$\mathbb{E}[\vec{\eta}(t) \otimes \vec{\eta}(t')]_{ij} = \Gamma_{ij} \delta_{ij} \delta(t - t') \quad [S-53]$$

265 δ_{ij} is the Kronecker delta.

266 With the uncorrelated noise assumption, the $\mathbb{V}[\vec{r}(t)]_{ij}$ can be expressed as follow, according equation (S-52):

$$\begin{aligned} \mathbb{V}[\vec{r}(t)]_{ij} &= \frac{1}{2m^2\gamma^3} (2\gamma t - 3 + 4e^{-\gamma t} - e^{-2\gamma t}) \begin{bmatrix} \Gamma_{xx} & 0 & 0 \\ 0 & \Gamma_{yy} & 0 \\ 0 & 0 & \Gamma_{zz} \end{bmatrix} \\ &= S(t) \begin{bmatrix} \Gamma_{xx} & 0 & 0 \\ 0 & \Gamma_{yy} & 0 \\ 0 & 0 & \Gamma_{zz} \end{bmatrix} \\ \mathbb{V}[\vec{r}(t)]_{ii} &= S(t) \Gamma_{ii} \end{aligned} \quad [S-54]$$

268 where $S(t)$ abbreviates for $\frac{1}{2m^2\gamma^3}(2\gamma t - 3 + 4e^{-\gamma t} - e^{-2\gamma t})$ in eq. (S-54).

269 Given the $\mathbb{E}[\vec{r}(t)]_i$ from eq. (S-48) and $\mathbb{V}[\vec{r}(t)]_{ii}$ from eq. (S-54), similar to eq. (S-29), the $\mathbb{P}(\vec{r}, t)$ can be expressed as follow:

$$\begin{aligned} \mathbb{P}(\vec{r}, t) &= \prod_i^{x,y,z} \mathcal{N}(r_i; \mu = \mathbb{E}[\vec{r}(t)]_i, \sigma^2 = \mathbb{V}[\vec{r}(t)]_{ii}) \\ &= \prod_i^{x,y,z} \mathcal{N}\left(r_i; \mu = r_{o,i} + \frac{v_{o,i}}{\gamma}(1 - e^{-\gamma t}), \sigma^2 = \Gamma_{ii}S(t)\right) \end{aligned} \quad \text{[S-55]}$$

271 The transition probability function

$$\mathbb{P}(\Delta\vec{r}, t_2, t_1) = \prod_i^{x,y,z} \mathcal{N}(\Delta r_i; \mu = \mathbb{E}[r_i(t_2)] - \mathbb{E}[r_i(t_1)], \sigma^2 = \Gamma_{ii}(S(t_2) - S(t_1))) \quad \text{[S-56]}$$

273 The $J_{ii}(t)$ and $\mathbb{E}[v_i(t)]$ can be expressed as:

$$\begin{aligned} J_{ii}(t) &= \frac{d}{dt}(\Gamma_{ii}S(t)) = \frac{\Gamma_{ii}}{m^2\gamma^2}(1 - e^{-\gamma t})^2 \\ \mathbb{E}[v_i(t)] &= \frac{d}{dt}(\mathbb{E}[r_i(t_2)]) = \frac{v_{o,i}}{\gamma}(1 - e^{-\gamma t}) \end{aligned} \quad \text{[S-57]}$$

275 Substituting $J_{ii}(t)$ and $\mathbb{E}[v_i(t)]$ to equation S-56, we have:

$$\mathbb{P}(\Delta\vec{r}, t_2, t_1) = \prod_i^{x,y,z} \mathcal{N}\left(\Delta r_i; \mu = \int_{t_1}^{t_2} \mathbb{E}[\vec{v}_i(t)] dt, \sigma^2 = \int_{t_1}^{t_2} J_{ii}(t) dt\right) \quad \text{[S-58]}$$

277 The two-time correlation function $c_1(\vec{q}, t_1, t_2)$ obtained through XPCS will be:

$$\begin{aligned} c_1(\vec{q}, t_1, t_2) &= \int_{-\infty}^{\infty} \mathbb{P}(\Delta\vec{r}, t_1, t_2) e^{i\vec{q}\cdot\Delta\vec{r}} d\Delta\vec{r} \\ &= \prod_i^{x,y,z} \int_{-\infty}^{\infty} \mathcal{N}\left(\Delta r_i; \mu = \int_{t_1}^{t_2} \mathbb{E}[v_i(t)] dt, \sigma^2 = \int_{t_1}^{t_2} J_{ii}(t) dt\right) e^{iq_i\Delta r_i} d\Delta r_i \\ &= \prod_i^{x,y,z} \int_{-\infty}^{\infty} \frac{1}{\sqrt{2\pi \int_{t_1}^{t_2} J_{ii}(t) dt}} \exp\left(-\frac{\left[\Delta r_i - \int_{t_1}^{t_2} \mathbb{E}[v_i(t)] dt\right]^2}{2 \int_{t_1}^{t_2} J_{ii}(t) dt} + iq_i\Delta r_i\right) d\Delta r_i \\ &= \prod_i^{x,y,z} e^{-\frac{1}{2}q_i^2 \int_{t_1}^{t_2} J_{ii}(t) dt} e^{iq_i \int_{t_1}^{t_2} \mathbb{E}[v_i(t)] dt} \\ &= e^{-\frac{1}{2} \int_{t_1}^{t_2} (q_x^2 J_{xx} + q_y^2 J_{yy} + q_z^2 J_{zz}) dt} e^{i \int_{t_1}^{t_2} q_x \mathbb{E}[v_x(t)] + q_y \mathbb{E}[v_y(t)] + q_z \mathbb{E}[v_z(t)] dt} \\ &= e^{-\frac{1}{2} \int_{t_1}^{t_2} (\vec{q} \cdot \underline{J}(t) \cdot \vec{q}) dt} e^{i\vec{q} \cdot \int_{t_1}^{t_2} \mathbb{E}[\vec{v}(t)] dt} \end{aligned} \quad \text{[S-59]}$$

279 where transport coefficient tensor \underline{J} is defined as:

$$\underline{J}(t) = \begin{bmatrix} J_{xx}(t) & 0 & 0 \\ 0 & J_{yy}(t) & 0 \\ 0 & 0 & J_{zz}(t) \end{bmatrix} \quad \text{[S-60]}$$

281 If we have assumed that the noise strength is isotropic ($\Gamma_{ii} = 2m\gamma k_B T$) and transport coefficient is the same for all the
282 components ($J = 3J_{xx} = 3J_{yy} = 3J_{zz}$) without external drive ($\mathbb{E}[v_x(t)] = \mathbb{E}[v_y(t)] = \mathbb{E}[v_z(t)] = 0$), based on equation S-57,
283 $c_1(\vec{q}, t_1, t_2)$ can be expressed as:

$$c_1(\vec{q}, t_1, t_2) = e^{-\frac{1}{6}(q_x^2 + q_y^2 + q_z^2) \int_{t_1}^{t_2} J(t) dt} \quad \text{[S-61]}$$

285 The term

$$q^2 = |\vec{q}|^2 = q_x^2 + q_y^2 + q_z^2 \quad \text{[S-62]}$$

287 defines an Ewald sphere in the reciprocal space where $c_1(\vec{q}, t_1, t_2)$ measured from any point in the sphere are equivalent in the
288 isotropic system.

289 In the Ornstein–Uhlenbeck process, assuming noise strength in each direction equals to the case in 1-dimension, $\Gamma_{ii} = 2m\gamma k_B T$,
 290 $J(t)$ can be expressed as:

$$291 \quad J(t) = 3J_{ii}(t) = 6 \frac{k_B T}{m\gamma} (1 - e^{-\gamma t})^2 \quad [\text{S-63}]$$

292 Substituting the diffusion constant defined as $D = \frac{k_B T}{m\gamma}$, the $J(t)$ is obtained as:

$$293 \quad J(t) = 6D(1 - e^{-\gamma t})^2 \quad [\text{S-64}]$$

294 As $t \rightarrow \infty$ where the system reaches equilibrium, $J(t)$ equals to

$$295 \quad J(t) = 6D \quad [\text{S-65}]$$

296 Based on the equation, we can conclude that, under the conditions of isotropic and uncorrelated noise, the transport
 297 coefficient $J(t)$ in 3-dimensional space is related to the transport coefficient in 1-dimension, $J_{ii}(t) = 2D$, as follows,

$$298 \quad J(t) = nJ_{ii}(t) \triangleq J_n(t) \quad [\text{S-66}]$$

299 where n stands for the number of dimensions in the system.

300 Therefore, substituting the equation S-66 to equation S-59, the $c_1(\vec{q}, t_1, t_2)$ in 3 dimensions with isotropic and uncorrelated
 301 noise in each direction can be expressed as:

$$302 \quad \begin{aligned} c_1(\vec{q}, t_1, t_2) &= e^{-\frac{1}{2}q^2 \int_{t_1}^{t_2} (nJ_{ii}(t)) dt} e^{i\vec{q} \cdot \int_{t_1}^{t_2} \mathbb{E}[\vec{v}(t)] dt} \\ &= e^{-\frac{1}{2}q^2 \int_{t_1}^{t_2} J_n(t) dt} e^{i\vec{q} \cdot \int_{t_1}^{t_2} \mathbb{E}[\vec{v}(t)] dt} \end{aligned} \quad [\text{S-67}]$$

303 Here, we expand the physical picture from 1 dimension to 3 dimensions. The equation S-67 is fundamental for further
 304 derivation for the equilibrium systems in complex fluid environments, such as laminar or shear banding flow.

305 E. $c_1(\vec{q}, t_1, t_2)$ in Homodyne Scattering.

306 **E.1. Generalized Equation for Homodyne Scattering.** In the combined XPCS and *in situ* Rheology (Rheo-XPCS) experiment, the
 307 laminar flow system can be conceptualized as comprising ensembles of flow layers across the gap ($0 \leq y \leq h$), each possessing
 308 the same transport coefficient $J(t)$ but different mean velocities $\mathbb{E}[\vec{v}(y, t)]$. The correlation function can be expressed as:

$$309 \quad \begin{aligned} c_1(\vec{q}, t_1, t_2) &= \sum_{y_1=1}^h \sum_{y_2=1}^h \frac{\Delta y_1}{h} \frac{\Delta y_2}{h} c_{1, y_1 - y_2}(\vec{q}, t_1, t_2) \\ &= \frac{1}{h^2} \sum_{y_1=1}^h \sum_{y_2=1}^h e^{-\frac{1}{2}q^2 \int_{t_1}^{t_2} J(t) dt} e^{i\vec{q} \cdot \int_{t_1}^{t_2} \mathbb{E}[\vec{v}(y_1, t)] - \mathbb{E}[\vec{v}(y_2, t)] dt} \Delta y_1 \Delta y_2 \\ &= \frac{1}{h^2} \int_0^h \int_0^h e^{-\frac{1}{2}q^2 \int_{t_1}^{t_2} J(t) dt} e^{i\vec{q} \cdot \int_{t_1}^{t_2} \mathbb{E}[\vec{v}(y_1, t)] - \mathbb{E}[\vec{v}(y_2, t)] dt} dy_1 dy_2 \end{aligned} \quad [\text{S-68}]$$

310 where $c_{1, y_1 - y_2}(\vec{q}, t_1, t_2)$ denotes as the correlation function between ensembles at position y_1 and y_2 in the gap.

311 Depending on its position in the gap (y) between the rotor and stator and taking into account the non-equilibrium nature of
 312 the system, where the shear rate changes over time, the velocity can be mathematically expressed as follows:

$$313 \quad \vec{v}(y, t) = v_x(y, t) = \dot{\gamma}(t)y \quad [\text{S-69}]$$

314 Based on the aforementioned equation, the particle mean displacement in Equation S-30 can be derived as follows:

$$315 \quad \int_{t_1}^{t_2} \mathbb{E}[\vec{v}(y, t)] dt = \int_{t_1}^{t_2} v_x(t) dt = y \int_{t_1}^{t_2} \dot{\gamma}(t) dt \quad [\text{S-70}]$$

316 In a homogeneous system with laminar flow that produces homodyne scattering, the integration of all the ensemble
 317 coordinates in Equation S-68 can be transformed from individual particles to spatial coordinates across the gap in the Couette
 318 geometry from 0 to h .

$$319 \quad \begin{aligned} c_1(\vec{q}, t_1, t_2) &= \frac{1}{h^2} \int_0^h \int_0^h e^{-\frac{1}{2}q^2 \int_{t_1}^{t_2} J(t) dt} e^{i\vec{q} \cdot \int_{t_1}^{t_2} \mathbb{E}[\vec{v}(y_1, t)] - \mathbb{E}[\vec{v}(y_2, t)] dt} dy_1 dy_2 \\ &= \left[e^{-\frac{1}{2}q^2 \int_{t_1}^{t_2} J(t) dt} \right] \frac{1}{h^2} \int_0^h \int_0^h e^{iq \int_{t_1}^{t_2} \dot{\gamma}(t) \cos(\phi(t)) dt} \Big|_{(y_1 - y_2)} dy_1 dy_2 \\ &= \left[e^{-\frac{1}{2}q^2 \int_{t_1}^{t_2} J(t) dt} \right] \text{sinc}^2 \left[\frac{1}{2}qh \int_{t_1}^{t_2} \dot{\gamma}(t) \cos(\phi(t)) dt \right] \end{aligned} \quad [\text{S-71}]$$

320 where ϕ is the angle between shear/flow direction and \vec{q} .

321 With Siegert Relation S-10, the $c_2(\vec{q}, t_1, t_2)$ can be expressed as:

$$322 \begin{aligned} c_2(\vec{q}, t_1, t_2) &= 1 + \beta |c_1(\vec{q}, t_1, t_2)|^2 \\ &= 1 + \beta \left[e^{-q^2 \int_{t_1}^{t_2} J(t) dt} \right] \text{sinc}^4 \left[\frac{1}{2} qh \int_{t_1}^{t_2} \dot{\gamma}(t) \cos(\phi(t)) dt \right] \end{aligned} \quad [\text{S-72}]$$

323 **E.2. Simplified Equation for Homodyne Scattering.** In the Rheo-XPCS experiment for system under strong deformation, the ensembles
324 at different positions exhibit a great difference in velocity. Therefore, eq. (S-68) is simplified by ignoring the cross-correlation
325 between different layers where $y_1 \neq y_2$,

$$326 \begin{aligned} c_1(\vec{q}, t_1, t_2) &= \sum_{y=y_1=y_2=1}^h \frac{\Delta y}{h} c_{1,y}(\vec{q}, t_1, t_2) = \frac{1}{h} \sum_{y=1}^h e^{-\frac{1}{2}q^2 \int_{t_1}^{t_2} J(t) dt} e^{i\vec{q} \cdot \int_{t_1}^{t_2} \mathbb{E}[\vec{v}(y,t)] dt} \Delta y \\ &= \frac{1}{h} \int_0^h e^{-\frac{1}{2}q^2 \int_{t_1}^{t_2} J(t) dt} e^{i\vec{q} \cdot \int_{t_1}^{t_2} \mathbb{E}[\vec{v}(y,t)] dt} dy \\ &= \left[e^{-\frac{1}{2}q^2 \int_{t_1}^{t_2} J(t) dt} \right] \frac{1}{h} \int_0^h e^{i \int_{t_1}^{t_2} \dot{\gamma}(t) \cos(\phi(t)) dt} dy \\ &= \left[e^{-\frac{1}{2}q^2 \int_{t_1}^{t_2} J(t) dt} \right] \text{sinc} \left[\frac{1}{2} qh \int_{t_1}^{t_2} \dot{\gamma}(t) \cos(\phi(t)) dt \right] e^{i \frac{1}{2} qh \int_{t_1}^{t_2} \dot{\gamma}(t) \cos(\phi(t)) dt} \end{aligned} \quad [\text{S-73}]$$

327 where ϕ is the angle between shear/flow direction and \vec{q} .

328 With Siegert Relation S-10, the $c_2(\vec{q}, t_1, t_2)$ can be expressed as:

$$329 \begin{aligned} c_2(\vec{q}, t_1, t_2) &= 1 + \beta |c_1(\vec{q}, t_1, t_2)|^2 \\ &= 1 + \beta \left[e^{-q^2 \int_{t_1}^{t_2} J(t) dt} \right] \text{sinc}^2 \left[\frac{1}{2} qh \int_{t_1}^{t_2} \dot{\gamma}(t) \cos(\phi(t)) dt \right] \end{aligned} \quad [\text{S-74}]$$

330 To consider the equilibrium condition of standard diffusion under constant shear where shear rate is constant as $\dot{\gamma}(t) \cos(\phi(t)) =$
331 $\dot{\gamma} \cos(\phi)$ and $J(t) = 6D$, the $c_2(\vec{q}, t_1, t_2)$ can be expressed as:

$$332 c_2(\vec{q}, t_1, t_2) = 1 + \beta \left[e^{-6q^2 D(t_2 - t_1)} \right] \text{sinc}^2 \left[\frac{1}{2} qh \cos(\phi) \dot{\gamma}(t_2 - t_1) \right] \quad [\text{S-75}]$$

333 Substituting the absolute time (t_2, t_1) by delayed time $\tau = t_2 - t_1$, the $c_2(\vec{q}, t_1, t_2)$ is reduced to the one-time correlation
334 function, $g_2(\vec{q}, \tau)$ as:

$$335 g_2(\vec{q}, \tau) = 1 + \beta \left[e^{-6q^2 D\tau} \right] \text{sinc}^2 \left[\frac{1}{2} qh \cos(\phi) \dot{\gamma}\tau \right] \quad [\text{S-76}]$$

336 The eq. (S-76) mentioned above is a commonly used homodyne equation that has been widely applied in various studies.

337 F. Systems with Multiple-Compositions in Non-Equilibrium.

338 **F.1. $c_2(\vec{q}, t_1, t_2)$ for Heterodyne Scattering with n -Compositions.** We can extend the analysis to include the time-dependent fraction
339 of each composition, $x_n(t)$. The total scattered electromagnetic wave, $E(\vec{q}, t)$, at a given time t can then be expressed as a
340 compositionally weighted contribution from the scattered electromagnetic fields of each composition, $E_n(\vec{q}, t)$, as follows:

$$341 \begin{aligned} E(\vec{q}, t) &= \sum_{n=1}^N x_n(t) E_n(\vec{q}, t) \\ 1 &= \sum_{n=1}^N x_n(t) \end{aligned} \quad [\text{S-77}]$$

342 The ensemble average intensity could be calculated as follows:

$$343 \begin{aligned} \mathbb{E}[I(\vec{q}, t)] &= \mathbb{E}[E(\vec{q}, t) E^*(\vec{q}, t)] \\ &= \mathbb{E} \left[\sum_{n=1}^N x_n(t) E_n(\vec{q}, t) \sum_{m=1}^N x_m(t) E_m^*(\vec{q}, t) \right] \\ &= \sum_{n=1}^N x_n^2(t) \mathbb{E}[|E_n(\vec{q}, t)|^2] + \sum_{n=1}^N \sum_{m \neq n}^N x_n(t) x_m(t) \mathbb{E}[E_n(\vec{q}, t) E_m^*(\vec{q}, t)] \end{aligned} \quad [\text{S-78}]$$

344 To simply the equation above, let's consider the following assumptions:

1. The average intensity produced by each scatterer is determined by a consistent unit scattering contrast, as all the scatterers are composed of the same materials. This unit scattering contrast remains constant across all scatterers and does not vary with time.

$$\mathbb{E}[I_n(\vec{q}, t)] = \mathbb{E}[|E_n(\vec{q}, t)|^2] = \mathbb{E}[|b|^2] \quad [\text{S-79}]$$

2. The electromagnetic field scattered from different compositions does not correlate with each other if the signals come from different compositions:

$$\sum_{n=1}^N \sum_{m \neq n}^N x_n(t) x_m(t) \mathbb{E}[E_n(\vec{q}, t) E_m(\vec{q}, t)] = 0 \quad [\text{S-80}]$$

With these two conditions, the average intensity could be written as

$$\mathbb{E}[I(\vec{q}, t)] = \mathbb{E}[|b|^2] \sum_{n=1}^N x_n(t)^2 \quad [\text{S-81}]$$

The correlation function between time t_1 and t_2 could be computed as:

$$c_1(\vec{q}, t_1, t_2) = \frac{\mathbb{E}[E(\vec{q}, t_2) E^*(\vec{q}, t_1)]}{[\mathbb{E}[|E(\vec{q}, t_1)|^2] \mathbb{E}[|E(\vec{q}, t_2)|^2]]^{\frac{1}{2}}} \quad [\text{S-82}]$$

Substituting the fractional relation eq. (S-77) to the previous correlation function:

$$\begin{aligned} c_1(\vec{q}, t_1, t_2) &= \frac{\mathbb{E}\left[\sum_{m=1}^N x_m(t_2) E_m(\vec{q}, t_2) \sum_{n=1}^N x_n(t_1) E_n^*(\vec{q}, t_1)\right]}{[\mathbb{E}[I(\vec{q}, t_1)] \mathbb{E}[I(\vec{q}, t_2)]]^{\frac{1}{2}}} \\ &= \frac{\left[\sum_{n=1}^N x_n(t_2) x_n(t_1) \mathbb{E}[E_n(\vec{q}, t_2) E_n^*(\vec{q}, t_1)] + \sum_{n=1}^N \sum_{m \neq n}^N x_m(t_2) x_n(t_1) \mathbb{E}[E_m(\vec{q}, t_2) E_n^*(\vec{q}, t_1)]\right]}{\left[\sum_{n=1}^N x_n(t_1)^2 \mathbb{E}[I_n(\vec{q}, t_1)] \sum_{n=1}^N x_n(t_2)^2 \mathbb{E}[I_n(\vec{q}, t_2)]\right]^{\frac{1}{2}}} \end{aligned} \quad [\text{S-83}]$$

The correlation function above could be interpreted as the sum of two components: the self-correlating terms for each component plus their cross-term. To simplify and rationalize the correlation function, we assume no spatial correlation of $E(\vec{q}, t)$ between scatterers in different composition ($n \neq m$) at different time:

$$\sum_{n=1}^N \sum_{m \neq n}^N x_n(t_1) x_m(t_2) \mathbb{E}[E_m(\vec{q}, t_2) E_n^*(\vec{q}, t_1)] = 0 \quad [\text{S-84}]$$

Now, introducing the compositional temporal correlation function, $c_{1,n}(\vec{q}, t_1, t_2)$, with form shown in eq. (S-67),

$$\begin{aligned} c_{1,n}(\vec{q}, t_1, t_2) &= \frac{\mathbb{E}[E_n(\vec{q}, t_2) E_n^*(\vec{q}, t_1)]}{[\mathbb{E}[|E_n(\vec{q}, t_2)|^2] \mathbb{E}[|E_n^*(\vec{q}, t_1)|^2]]^{\frac{1}{2}}} = \frac{\mathbb{E}[E_n(\vec{q}, t_2) E_n^*(\vec{q}, t_1)]}{\mathbb{E}[I(\vec{q}, t)]} \\ &= e^{-\frac{1}{2}q^2 \int_{t_1}^{t_2} J_n(t) dt} e^{i\vec{q} \cdot \int_{t_1}^{t_2} \mathbb{E}[\vec{v}_n(t)] dt} \end{aligned} \quad [\text{S-85}]$$

the self-correlation part of $c_1(\vec{q}, t_1, t_2)$ can be written as follows:

$$\begin{aligned} \sum_{n=1}^N x_n(t_1) x_n(t_2) \mathbb{E}[E_n(\vec{q}, t_2) E_n^*(\vec{q}, t_1)] &= \mathbb{E}[I(\vec{q}, t)] \sum_{n=1}^N x_n(t_1) x_n(t_2) c_{1,n}(\vec{q}, t_1, t_2) \\ &= \mathbb{E}[|b|^2] \sum_{n=1}^N x_n(t_1) x_n(t_2) e^{-\frac{1}{2}q^2 \int_{t_1}^{t_2} J_n(t) dt} e^{i\vec{q} \cdot \int_{t_1}^{t_2} \mathbb{E}[\vec{v}_n(t)] dt} \end{aligned} \quad [\text{S-86}]$$

366 The correlation function thus could be simplified as:

$$\begin{aligned}
c_1(\vec{q}, t_1, t_2) &= \frac{\mathbb{E} [|b|^2] \sum_{n=1}^N x_n(t_1)x_n(t_2)c_{1,n}(\vec{q}, t_1, t_2)}{\mathbb{E} [|b|^2] \left[\sum_{n=1}^N x_n(t_1)^2 \sum_{n=1}^N x_n(t_2)^2 \right]^{\frac{1}{2}}} \\
&= \frac{\sum_{n=1}^N x_n(t_1)x_n(t_2)c_{1,n}(\vec{q}, t_1, t_2)}{\left[\sum_{n=1}^N x_n(t_1)^2 \sum_{n=1}^N x_n(t_2)^2 \right]^{\frac{1}{2}}} \\
&= \frac{1}{f} \sum_{n=1}^N x_n(t_1)x_n(t_2)c_{1,n}(\vec{q}, t_1, t_2) \\
&= \frac{1}{f} \sum_{n=1}^N x_n(t_1)x_n(t_2) e^{-\frac{1}{2}q^2 \int_{t_1}^{t_2} J_n(t) dt} e^{i\vec{q} \cdot \int_{t_1}^{t_2} \mathbb{E}[\vec{v}_n(t)] dt}
\end{aligned} \tag{S-87}$$

368 Let the normalization factor f define as $f = \left[\sum_{n=1}^N x_n(t_1)^2 \sum_{n=1}^N x_n(t_2)^2 \right]^{\frac{1}{2}}$.

369 We then apply the Siegert relation S-10 to obtain the $c_2(\vec{q}, t_1, t_2)$ function measured from the XPCS experiment under
370 speckle contrast of β :

$$\begin{aligned}
c_2(\vec{q}, t_1, t_2) &= 1 + \beta |c_1(\vec{q}, t_1, t_2)|^2 \\
&= 1 + \beta [c_1(\vec{q}, t_1, t_2)c_1^*(\vec{q}, t_1, t_2)] \\
&= 1 + \beta \left[\sum_{n=1}^N x_n(t_1)x_n(t_2)c_{1,n} \sum_{m=1}^N x_m(t_1)x_m(t_2)c_{1,m}^* \right] \\
&= 1 + \frac{\beta}{f^2} \sum_{n=1}^N \sum_{m=1}^N x_n(t_1)x_n(t_2)x_m(t_1)x_m(t_2)c_{1,n}c_{1,m}^*
\end{aligned} \tag{S-88}$$

372 Subsequently, $c_2(\vec{q}, t_1, t_2)$ is obtained by substituting from equation S-85:

$$c_2(\vec{q}, t_1, t_2) = 1 + \frac{\beta}{f^2} \sum_{n=1}^N \sum_{m=1}^N \left[\begin{array}{l} x_n(t_1)x_n(t_2)x_m(t_1)x_m(t_2) \times \\ e^{-\frac{1}{2}q^2 \int_{t_1}^{t_2} J_n(t)+J_m(t) dt} \times \\ e^{i\vec{q} \cdot \int_{t_1}^{t_2} \mathbb{E}[\vec{v}_n(t)] - \mathbb{E}[\vec{v}_m(t)] dt} \end{array} \right] \tag{S-89}$$

374 In the XPCS experiment, only the real part in the eq. (S-89) can be observed:

$$\begin{aligned}
c_2(\vec{q}, t_1, t_2) &= 1 + \frac{\beta}{f^2} \sum_{n=1}^N \sum_{m=1}^N \mathbf{Re} \left[\begin{array}{l} x_n(t_1)x_n(t_2)x_m(t_1)x_m(t_2) \times \\ e^{-\frac{1}{2}q^2 \int_{t_1}^{t_2} J_n(t)+J_m(t) dt} \times \\ e^{i\vec{q} \cdot \int_{t_1}^{t_2} \mathbb{E}[\vec{v}_n(t)] - \mathbb{E}[\vec{v}_m(t)] dt} \end{array} \right] \\
&= 1 + \frac{\beta}{f^2} \sum_{n=1}^N \sum_{m=1}^N \left[\begin{array}{l} x_n(t_1)x_n(t_2)x_m(t_1)x_m(t_2) \times \\ e^{-\frac{1}{2}q^2 \int_{t_1}^{t_2} J_n(t)+J_m(t) dt} \times \\ \mathbf{Re} \left[e^{i\vec{q} \cdot \int_{t_1}^{t_2} \mathbb{E}[\vec{v}_n(t)] - \mathbb{E}[\vec{v}_m(t)] dt} \right] \end{array} \right]
\end{aligned} \tag{S-90}$$

376 The term \mathbf{Re} denotes taking the real part from the complex term of $e^{i\vec{q} \cdot \int_{t_1}^{t_2} \mathbb{E}[\vec{v}_n(t)] - \mathbb{E}[\vec{v}_m(t)] dt}$, the cosine part,

$$\mathbf{Re} \left[e^{i\vec{q} \cdot \int_{t_1}^{t_2} \mathbb{E}[\vec{v}_n(t)] - \mathbb{E}[\vec{v}_m(t)] dt} \right] = \cos \left[\vec{q} \cdot \int_{t_1}^{t_2} \mathbb{E}[\vec{v}_n(t)] - \mathbb{E}[\vec{v}_m(t)] dt \right] \tag{S-91}$$

378 For the self-interference part as $n = m$, this term equalizes to 1:

$$\begin{aligned}
\mathbf{Re} \left[e^{i\vec{q} \cdot \int_{t_1}^{t_2} \mathbb{E}[\vec{v}_n(t)] - \mathbb{E}[\vec{v}_n(t)] dt} \right] &= \cos \left[\vec{q} \cdot \int_{t_1}^{t_2} \mathbb{E}[\vec{v}_n(t)] - \mathbb{E}[\vec{v}_n(t)] dt \right] \\
&= \cos [0] = 1
\end{aligned} \tag{S-92}$$

380 As we further consider that the displacement of each composition is attributed to the flow along direction $\phi_n(t)$ relative to
 381 scattering vector \vec{q} , the interference term can be simplified as:

$$382 \quad \mathbf{Re} \left[e^{i\vec{q} \cdot \int_{t_1}^{t_2} \mathbb{E}[\vec{v}_n(t)] - \mathbb{E}[\vec{v}_m(t)] dt} \right] = \cos \left[q \int_{t_1}^{t_2} \mathbb{E}[v_n(t)] \cos(\phi_n(t)) - \mathbb{E}[v_m(t)] \cos(\phi_m(t)) dt \right] \quad \text{[S-93]}$$

383 The completed form of the time correlation function with heterodyne scattering under time-dependent change in fraction
 384 and relative velocity is written as follows:

$$385 \quad c_2(\vec{q}, t_1, t_2) = 1 + \frac{\beta}{f^2} \sum_{n=1}^N \sum_{m=1}^N \left[\begin{array}{c} x_n(t_1)x_n(t_2)x_m(t_1)x_m(t_2) \times \\ e^{-\frac{1}{2}q^2 \int_{t_1}^{t_2} J_n(t) + J_m(t) dt} \times \\ \cos \left[q \int_{t_1}^{t_2} \mathbb{E}[v_n(t)] \cos(\phi_n(t)) - \mathbb{E}[v_m(t)] \cos(\phi_m(t)) dt \right] \end{array} \right] \quad \text{[S-94]}$$

386 **F.2. Heterodyne Scattering with 2 Compositions.** To verify the equation in general form, we consider a simpler case. In this context,
 387 the heterodyne equation in the system with 2 compositions, static reference (r) and sample (s), consistently moving with
 388 relative speed $\mathbb{E}[v]$ and direction ϕ concerning scattering vector \vec{q} , the equation could be simplified as:

$$389 \quad c_2(\vec{q}, t_1, t_2) = 1 + \frac{\beta}{f^2} \left[\begin{array}{c} [x_r(t_1)x_r(t_2)]^2 e^{-q^2 \int_{t_1}^{t_2} J_r(t) dt} + \\ [x_s(t_1)x_s(t_2)]^2 e^{-q^2 \int_{t_1}^{t_2} J_s(t) dt} + \\ 2x_r(t_1)x_r(t_2)x_s(t_1)x_s(t_2) e^{-\frac{1}{2}q^2 \int_{t_1}^{t_2} J_s(t) + J_r(t) dt} \cos \left[q \cos(\phi) \int_{t_1}^{t_2} \mathbb{E}[v] dt \right] \end{array} \right] \quad \text{[S-95]}$$

$$f^2 = [x_s(t_1)^2 + x_r(t_1)^2] [x_s(t_2)^2 + x_r(t_2)^2]$$

390 To further consider the equilibrium conditions in the Wiener process or standard diffusion, in which all parameters, including
 391 x_s , x_r and v , are independent of time and $J_n(t) = 6D_n$, the equation could be further simplified as:

$$392 \quad c_2(\vec{q}, t_1, t_2) = 1 + \frac{\beta}{f^2} \left[\begin{array}{c} x_r^4 e^{-6q^2 D_r(t_2-t_1)} + x_s^4 e^{-6q^2 D_s(t_2-t_1)} + \\ 2x_r^2 x_s^2 e^{-3q^2(D_r+D_s)(t_2-t_1)} \cos [q \cos(\phi) \mathbb{E}[v] (t_2 - t_1)] \end{array} \right] \quad \text{[S-96]}$$

$$f^2 = [x_s^2 + x_r^2]^2$$

393 Further apply the condition for the composition (x) and delayed time (τ):

$$394 \quad x = \frac{I_s}{I_s + I_r} = \frac{x_s^2 \mathbb{E}[I]}{x_s^2 \mathbb{E}[I] + x_r^2 \mathbb{E}[I]} = \frac{x_s^2}{x_s^2 + x_r^2} = \frac{x_s^2}{f} \quad \text{[S-97]}$$

$$\tau = t_2 - t_1$$

395 The one-time correlation equation for heterodyne scattering $g_2(\vec{q}, \tau)$ is shown as:

$$396 \quad g_2(\vec{q}, \tau) = 1 + \beta \left[\begin{array}{c} (1-x)^2 e^{-6q^2 D_r \tau} + x^2 e^{-6q^2 D_s \tau} + \\ 2x(1-x) e^{-3q^2(D_r+D_s)\tau} \cos [q \cos(\phi) \mathbb{E}[v] \tau] \end{array} \right] \quad \text{[S-98]}$$

397 The equation S-98 above is a commonly used heterodyne equation that has been widely applied in various studies.

398 **F.3. Heterodyne Scattering with 3 compositions.** We further consider a system constituted of 3 compositions with 2 flowing components
 399 as (1, 2) and 1 static component as (r). The flowing composition moves with velocity (v_1, v_2) and direction (ϕ_1, ϕ_2) relative to
 400 the \vec{q} . The heterodyne equation could be expressed as follows:

$$401 \quad c_2(\vec{q}, t_1, t_2) = 1 + \frac{\beta}{f(t_1, t_2)^2} [c_{2,self} + c_{2,cross}] \quad \text{[S-99]}$$

402 with the normalization factor written as:

$$403 \quad f(t_1, t_2)^2 = [x_1(t_1)^2 + x_2(t_1)^2 + x_r(t_1)^2] [x_1(t_2)^2 + x_2(t_2)^2 + x_r(t_2)^2] \quad \text{[S-100]}$$

404 and $c_{2,self}$ and $c_{2,cross}$ denoted as the self-correlation and cross-correlation between different compositions, respectively. These
 405 correlation functions are defined as follows:

$$\begin{aligned}
c_{2,self} &= \begin{bmatrix} [x_r(t_1)x_r(t_2)]^2 e^{-q^2 \int_{t_1}^{t_2} J_r(t) dt} + \\ [x_1(t_1)x_1(t_2)]^2 e^{-q^2 \int_{t_1}^{t_2} J_1(t) dt} + \\ [x_2(t_1)x_2(t_2)]^2 e^{-q^2 \int_{t_1}^{t_2} J_2(t) dt} + \end{bmatrix} \\
c_{2,cross} &= \begin{bmatrix} 2x_r(t_1)x_r(t_2)x_1(t_1)x_1(t_2)e^{-\frac{1}{2}q^2 \int_{t_1}^{t_2} J_r(t)+J_1(t) dt} \times \\ \cos \left[q \int_{t_1}^{t_2} \mathbb{E} [v_1(t)] \cos(\phi_1(t)) dt \right] + \\ 2x_r(t_1)x_r(t_2)x_2(t_1)x_2(t_2)e^{-\frac{1}{2}q^2 \int_{t_1}^{t_2} J_r(t)+J_2(t) dt} \times \\ \cos \left[q \int_{t_1}^{t_2} \mathbb{E} [v_2(t)] \cos(\phi_2(t)) dt \right] + \\ 2x_1(t_1)x_1(t_2)x_2(t_1)x_2(t_2)e^{-\frac{1}{2}q^2 \int_{t_1}^{t_2} J_2(t)+J_1(t) dt} \times \\ \cos \left[q \int_{t_1}^{t_2} \mathbb{E} [v_1(t)] \cos(\phi_1(t)) - \mathbb{E} [v_2(t)] \cos(\phi_2(t)) dt \right] \end{bmatrix}
\end{aligned} \tag{S-101}$$

The equation shown above represents the heterodyne scattering function for a system with three components, and its calculation involves a large number of parameters. Due to the complexity of this calculation, it becomes challenging to directly extract the physical parameters from the measured data using this equation. To overcome this difficulty, it is necessary to employ approximations based on the specific characteristics of the physical system. The following approximations are commonly utilized:

1. The intrinsic dynamics of the reference position is much slower than that of the flowing composition as $J_r = 0$ and, therefore, $c_{1,r} = 1$.
2. The flow direction of each composition is dominated at the horizontal direction and, therefore, $\phi_1 = \phi_2 = \theta$, where θ is the angle between \vec{q} and the horizontal reference of $\theta = 0$.

With all the reasonable assumptions above, the final form of the heterodyne scattering function for 3 flowing bands, which will be utilized for analysis in this paper, is as follows:

$$\begin{aligned}
c_{2,self} &= \begin{bmatrix} [x_r(t_1)x_r(t_2)]^2 + \\ [x_1(t_1)x_1(t_2)]^2 e^{-q^2 \int_{t_1}^{t_2} J_1(t) dt} + \\ [x_2(t_1)x_2(t_2)]^2 e^{-q^2 \int_{t_1}^{t_2} J_2(t) dt} + \end{bmatrix} \\
c_{2,cross} &= \begin{bmatrix} 2x_r(t_1)x_r(t_2)x_1(t_1)x_1(t_2)e^{-\frac{1}{2}q^2 \int_{t_1}^{t_2} J_1(t) dt} \times \\ \cos \left[q \cos(\theta) \int_{t_1}^{t_2} \mathbb{E} [v_1(t)] dt \right] + \\ 2x_r(t_1)x_r(t_2)x_2(t_1)x_2(t_2)e^{-\frac{1}{2}q^2 \int_{t_1}^{t_2} J_2(t) dt} \times \\ \cos \left[q \cos(\theta) \int_{t_1}^{t_2} \mathbb{E} [v_2(t)] dt \right] + \\ 2x_1(t_1)x_1(t_2)x_2(t_1)x_2(t_2)e^{-\frac{1}{2}q^2 \int_{t_1}^{t_2} J_2(t)+J_1(t) dt} \times \\ \cos \left[q \cos(\theta) \int_{t_1}^{t_2} \mathbb{E} [v_1(t)] - \mathbb{E} [v_2(t)] dt \right] \end{bmatrix}
\end{aligned} \tag{S-102}$$

3. Formalization of Physical Parameters

A. Analysis in Fig. 3 Panels C and D. In an ideal situation of a non-equilibrium model, various time-dependent parameters $p(t)$ within the model, such as $J(t)$, $\dot{\gamma}(t)$ and $\mathbb{E}[v(t)]$, should be continuous arbitrary where each frame of t corresponds to a specific value. Consequently, to accurately capture the dynamics evolution over time, the fitting process should involve thousands of parameters that correspond to each measured frame, as follows:

$$p(t) : p(t=0), p(1), p(2) \cdots \cdots p(t) \tag{S-103}$$

This analysis approach is employed in the results shown in Fig. 3 Panels C and D of the manuscript. However, when practically analyzing extended time procedures, for the sake of streamlining the fitting process and minimizing the parameter count, these time-dependent parameters can be effectively approximated using various functions.

B. Analysis in Fig. 2. In the analysis of our Molecular Dynamics (MD) simulation, where the system is homogeneous and the temperature exhibits a smooth transition from high to low, the trend of the $J(t)$ is represented by the error function (erfc) as follow:

$$J(t) = J_{scale} \text{erfc}(t_{scale}(t - t_{shift})) + J_{shift} \tag{S-104}$$

which J_{scale} , J_{shift} , t_{scale} and t_{shift} are parameters to either stretch or shift the error function in different axis to accommodate the actual change of $J(t)$ along time.

434 **C. Analysis in Fig. 3 Panels A and B.** To more effectively model the intrinsic dynamics observed during the relaxation process
 435 using a simplified approach, we have represented the trend of $J(t)$ through a power law that incorporates three parameters:
 436 the scale factor (J_o), the exponent (b), and a vertical shift (D_o),

$$437 \quad J(t) = J_o t^b + D_o \quad [S-105]$$

438 was utilized to formalize the relation between $J(t)$ and time t . In Equation (S-105), J_o represents the scaling of the transport
 439 coefficient, and D_o signifies the intrinsic diffusion rate of the system at equilibrium. The exponent b delineates the power-law
 440 behavior.

441 **D. Analysis in Fig. 4.** In the analysis of multiple-banding system, the function of the physical parameters for the two flowing
 442 components, including mean velocity $v_1(t)$ and $v_2(t)$, transport coefficient $J_1(t)$ and $J_2(t)$, and fraction $x_1(t)$ and $x_2(t)$, are
 443 divided into 2 segments at $t = 15$ when the dynamics process changes its trend. This segmentation in the dynamics analysis
 444 arises from the non-monotonic behavior observed in the variables $J(t), v$, and x_n , where each displays a pattern of increase
 445 followed by a decrease. Such trends complicate the use of a single function to precisely capture these variations accurately.
 446 Consequently, second order two-time intensity autocorrelation function (c_2) was segmented into two parts at the $t = 15s$, each
 447 modeled by distinct functions. To describe v_1 and v_2 , $J_1(t)$ and $J_2(t)$ at different segments, a power law is utilized as:

$$448 \quad \begin{aligned} J_1(t) &= \begin{cases} a_{J,1,1} t^{b_{J,1,1}} + c_{J,1,1} & : t < 15 \\ a_{J,1,2} t^{b_{J,1,2}} + c_{J,1,2} & : t \geq 15 \end{cases} \\ J_2(t) &= \begin{cases} a_{J,2,1} t^{b_{J,2,1}} + c_{J,2,1} & : t < 15 \\ a_{J,2,2} t^{b_{J,2,2}} + c_{J,2,2} & : t \geq 15 \end{cases} \\ v_1(t) &= \begin{cases} a_{v,1,1} t^{b_{v,1,1}} + c_{v,1,1} & : t < 15 \\ a_{v,1,2} t^{b_{v,1,2}} + c_{v,1,2} & : t \geq 15 \end{cases} \\ v_2(t) &= \begin{cases} a_{v,2,1} t^{b_{v,2,1}} + c_{v,2,1} & : t < 15 \\ a_{v,2,2} t^{b_{v,2,2}} + c_{v,2,2} & : t \geq 15 \end{cases} \end{aligned} \quad [S-106]$$

449 where scale (a), exponent (b), and vertical shift (c) are fitting parameters of the power law and labeled by subscript corresponding
 450 to its (Parameters, Segment, Component).

451 Additional constraints are imposed on the fitting process for $x_1(t)$ and $x_2(t)$, taking into account the inherent limits of
 452 fraction growth and reduction, which are confined within the range of 0 and 1.

$$453 \quad \begin{aligned} x_1(t) &= \begin{cases} d_{x,1,1} - a_{x,1,1} e^{b_{x,1,1}(t-c_{x,1,1})} & : t < 15 \\ a_{x,1,2} e^{b_{x,1,2}(t-c_{x,1,2})} & : t \geq 15 \end{cases} \\ x_2(t) &= \begin{cases} d_{x,2,1} - a_{x,2,1} e^{b_{x,2,1}(t-c_{x,2,1})} & : t < 15 \\ a_{x,2,2} e^{b_{x,2,2}(t-c_{x,2,2})} & : t \geq 15 \end{cases} \end{aligned} \quad [S-107]$$

454 Any negative values in $x_1(t)$ and $x_2(t)$ is substituted by 0.

455 The interpretation of the physical parameters in these model functions could vary depending on the specific context of their
 456 application. For instance, b_n in S-105 could relate to the exponent that characterizes the time dependency of the dynamics rate
 457 as $\dot{\gamma} \sim t^{b_n}$ when it is extracted from a system undergoes relaxations or deformations.

458 4. Application in Model Systems

459 **A. Classical Non-Equilibrium Dynamics Model.** In the following section, we apply equation S-67 to several classical processes
 460 that match the description of Langevin dynamics, including the Wiener process (standard diffusion), Ornstein–Uhlenbeck
 461 process, and Brownian oscillator. By analyzing these dynamic processes, we can estimate the transport coefficients and,
 462 hopefully, gain insight into how this physical parameter represents the dynamic behavior of the system.

463 **A.1. Wiener Process / Standard Diffusion.** In this case of 1-dimensional Wiener process or standard diffusion, fluctuations ($\zeta(t)$)
 464 exist at the velocity level as $\Gamma = 2D$. Under such conditions, the Langevin equation of the Wiener process can be expressed as
 465 (3, at eq. (9.2)):

$$466 \quad \dot{x} = v_o + R(t) = v_o + \sqrt{2D}\zeta(t) \quad [S-108]$$

467 Here, $R(t)$ represents a random fluctuation in velocity attributed to a stationary, Gaussian, δ -correlated, Markov process
 468 $\zeta(t)$. It possesses the following properties:

$$469 \quad \mathbb{E} [\zeta(t)\zeta(t')] = \delta(t - t') \quad [S-109]$$

470 where v_o and x_0 are the initial velocity and position for the process.

471 The mean velocity $\mathbb{E}[v(t)]$, mean position $\mathbb{E}[x(t)]$, variance of position $\mathbb{V}[x(t)]$ and transport coefficient $J(t)$ of the ensemble
472 are obtained as:

$$\begin{aligned}
\mathbb{E}[v(t)] &= v_o \\
\mathbb{E}[v(t)v(t')] &= v_o^2 + 2D\delta(t-t') \\
\mathbb{E}[x(t)] &= x_0 + v_o t \\
\mathbb{V}[x(t)] &= \mathbb{E}[x(t)^2] - \mathbb{E}[x(t)]^2 = 2Dt \\
J(t) &= \frac{d}{dt}(\mathbb{V}[x(t)]) = 2D
\end{aligned}
\tag{S-110}$$

474 Substituting the value of $\mathbb{E}[v(t)]$ and $\mathbb{V}[x(t)]$ from equation S-110 to equation S-40, the $c_1(q, t_1, t_2)$ is obtained based on as:

$$c_1(q, t_1, t_2) = e^{-q^2 D(t_2 - t_1)} e^{iqv_o(t_2 - t_1)} \tag{S-111}$$

476 Equation (S-111) is the $c_1(q, t_1, t_2)$ for the model of Advection-Diffusion in 1-dimension, a fluid transports with external
477 driven bulk movement (v_o) and diffusion (D) of the substance due to molecular random motion.

478 Considering the case in equilibrium state as changing the absolute time (t_1, t_2) to delayed time τ as $\tau = t_2 - t_1$:

$$g_1(q, \tau) = e^{-q^2 D\tau} e^{iqv_o\tau} \tag{S-112}$$

480 Further considering diffusion is the only dynamics in the system and there is no bulk movement in the system as $v_o = 0$, the
481 equation S-112 can be reduced to the simplest model that commonly applied in XPCS analysis:

$$g_1(q, \tau) = e^{-q^2 D\tau} \tag{S-113}$$

483 **A.2. Ornstein–Uhlenbeck Process.** In **Ornstein–Uhlenbeck Process**, the external force (F_{ex}) is set to zero while the drift
484 coefficient (γ) remains non-zero. This configuration gives rise to an Ornstein–Uhlenbeck process. The Ornstein–Uhlenbeck
485 process exhibits a mean-reverting behavior and is commonly used to model systems with a tendency to return to equilibrium.
486 In such a case, the Langevin equation is given by (3, at eq. (6.1)):

$$m\dot{v} = -m\gamma v(t) + \eta(t) \tag{S-114}$$

488 In the Ornstein–Uhlenbeck process, the thermal fluctuation noise in velocity is attributed to collisions between particles and
489 solvent with the level of $\Gamma = 2m\gamma k_B T$. Then, the mean velocity $\mathbb{E}[v(t)]$, mean position $\mathbb{E}[x(t)]$ and variance of position $\mathbb{V}[x(t)]$
490 of the ensemble is solved as:

$$\begin{aligned}
\mathbb{E}[v(t)] &= v_o e^{-\gamma t} \\
\mathbb{E}[x(t)] &= x_0 + \frac{v_o}{\gamma} (1 - e^{-\gamma t}) \\
\mathbb{V}[x(t)] &= \mathbb{E}[x(t)^2] - \mathbb{E}[x(t)]^2 = \frac{k_B T}{m\gamma^2} (2\gamma t - 3 + 4e^{-\gamma t} - e^{-2\gamma t}) \\
&= \frac{D}{\gamma} (2\gamma t - 3 + 4e^{-\gamma t} - e^{-2\gamma t})
\end{aligned}
\tag{S-115}$$

492 where D is defined as the diffusion constant of the system and is equal to $D = \frac{k_B T}{m\gamma}$

493 The dynamical transport coefficient $J(t)$ is defined as:

$$\begin{aligned}
J(t) &= \frac{d}{dt}(\mathbb{V}[x(t)]) = \frac{d}{dt} \left(\frac{D}{\gamma} (2\gamma t - 3 + 4e^{-\gamma t} - e^{-2\gamma t}) \right) \\
&= 2D(1 - 2e^{-\gamma t} + e^{-2\gamma t}) \\
&= 2D(1 - e^{-\gamma t})^2
\end{aligned}
\tag{S-116}$$

495 The two-time correlation function $c_1(q, t_1, t_2)$ obtained through XPCS will be:

$$\begin{aligned}
c_1(q, t_1, t_2) &= e^{-\frac{1}{2}q^2 \int_{t_1}^{t_2} J(t) dt} e^{iq \int_{t_1}^{t_2} \mathbb{E}[v(t)] dt} \\
&= e^{-q^2 D \int_{t_1}^{t_2} (1 - e^{-\gamma t})^2 dt} e^{iqv_o \int_{t_1}^{t_2} \exp(-\gamma t) dt}
\end{aligned}
\tag{S-117}$$

497 **A.3. Brownian Oscillator.** In a Brownian oscillator with potential of $V(x) = \frac{1}{2}m\omega_o^2 x^2$, the conservative force in the particle is
 498 $m\omega_o^2 x$ as $-\frac{\partial V(x)}{\partial x} = -m\omega_o^2 x$. Therefore, the Langevin Equation (LE) for the Brownian oscillator is: (3, at eq. (13.1))

$$499 \quad m\dot{v} = -m\gamma v + \eta(t) - m\omega_o^2 x \quad [\text{S-118}]$$

500 For the Brownian oscillator with initial conditions of $x(0) = x_o$ and $v(0) = v_o$, the value of $\mathbb{E}[v(t)]$, $\mathbb{E}[x(t)]$ and $\mathbb{V}[x(t)]$ is
 501 solved as: (5, at eq. (214))

$$\begin{aligned} \mathbb{E}[v(t)] &= \frac{e^{-\gamma t/2}}{\omega_s} \left[-x_o(\omega_o^2 \sin \omega_s t) + v_o(\omega_s \cos \omega_s t - \frac{1}{2}\gamma \sin \omega_s t) \right] \\ \mathbb{E}[x(t)] &= \frac{e^{-\gamma t/2}}{\omega_s} \left[x_o(\omega_s \cos \omega_s t + \frac{1}{2}\gamma \sin \omega_s t) + v_o(\sin \omega_s t) \right] \\ \mathbb{V}[x(t)] &= \frac{k_B T}{m\omega_o^2} \left[1 - e^{-\gamma t} \left(\frac{\gamma^2}{2\omega_s^2} \sin^2 \omega_s t + \frac{\gamma}{2\omega_s} \sin 2\omega_s t + 1 \right) \right] \end{aligned} \quad [\text{S-119}]$$

503 where ω_s is the reduced frequency given as:

$$504 \quad \omega_s = \left(\omega_o^2 - \frac{1}{4}\gamma^2 \right)^{\frac{1}{2}} \quad [\text{S-120}]$$

505 With the knowledge of $\mathbb{V}[x(t)]$ and $\mathbb{V}[v(t)]$, the transport coefficient $J(t)$ for Brownian oscillator can be written as: (5, at eq.
 506 (213))

$$507 \quad J(t) = \frac{d}{dt} (\mathbb{V}[x(t)]) = \frac{2D\gamma^2}{\omega_s^2} e^{-\gamma t} \sin^2 \omega_s t \quad [\text{S-121}]$$

508 Substituting the value of $\mathbb{E}[v(t)]$ and $J(t)$ from equations S-119 and S-121 to equation S-40, the two-time correlation function
 509 for XPCS, $c_1(t_1, t_2)$, becomes,

$$\begin{aligned} c_1(q, t_1, t_2) &= e^{-\frac{1}{2}q^2 \int_{t_1}^{t_2} J dt} e^{iq \int_{t_1}^{t_2} \mathbb{E}[v(t)] dt} \\ &= \exp \left(-\frac{D\gamma^2 q^2}{\omega_s^2} \int_{t_1}^{t_2} e^{-\gamma t} \sin^2 \omega_s t dt \right) \\ &\quad \times \exp \left(i \frac{q e^{-\gamma t/2}}{\omega_s} \int_{t_1}^{t_2} -x_o(\omega_o^2 \sin \omega_s t) + v_o(\omega_s \cos \omega_s t - \frac{1}{2}\gamma \sin \omega_s t) dt \right) \end{aligned} \quad [\text{S-122}]$$

511 **B. Analysis in Transport Coefficient.** As delineated in section 3, if the internal and external forces, such as conservative forces
 512 or hydrodynamic forces, are described by complicated functions, $J(t)$ and $\mathbb{V}[x(t)]$ are not analytically solvable. Therefore, we
 513 propose to extract $J(t)$ with arbitrary profile functions (e.g., eq. (S-104)) to capture non-equilibrium dynamics in such systems.
 514 However, the physical interpretation of $J(t)$ and $\mathbb{V}[x(t)]$ are not clear. On the other hand, throughout the derivations in the
 515 previous section A, the $J(t)$ and $\mathbb{V}[x(t)]$ are analytically resolved from the Langevin equation for well-defined models of the
 516 Wiener process, Ornstein-Uhlenbeck process, and Brownian oscillator. Below, we will show that the estimation of $J(t)$ and
 517 $\mathbb{V}[x(t)]$ from these models facilitates a better understanding of their physics.

518 **B.1. Wiener Process / Standard Diffusion.** For Wiener process, $J(t)$ is obtained as:

$$519 \quad J(t) = 2D \quad [\text{S-123}]$$

520 Since there are no drift or external forces applied to the particles, the system is in equilibrium and the dynamics of the
 521 particles are independent of time. Therefore, the obtained $J(t)$ correlates with the diffusion constant.

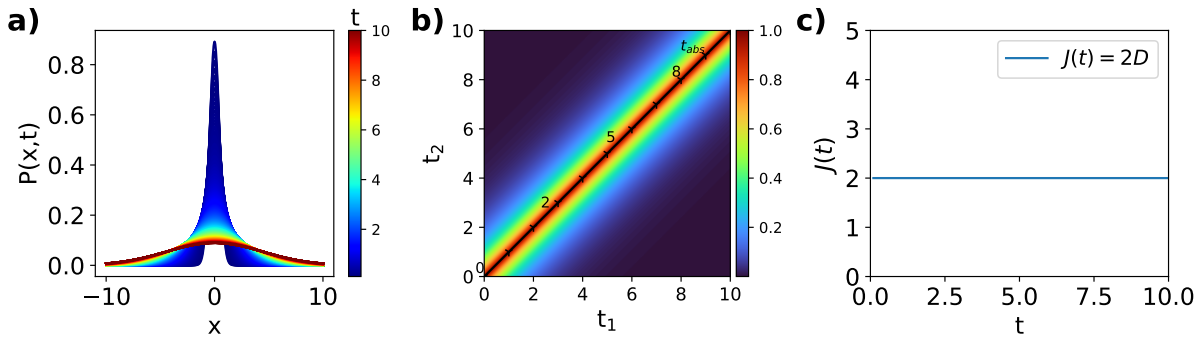


Fig. S1. Simulation for Wiener Process / Standard Diffusion with $D = 1$ and $x_o = 0$. a) $P(x, t)$ represents the probability density function as time evolves. b) The figure illustrates the two-time correlation function, $c_2(q = 1, t_1, t_2)$. c) $J(t)$ is the transport coefficient described in this work. In such an equilibrium state, the dynamical transport coefficient $J(t) = 2D$ is independent of time.

522 **B.2. Ornstein–Uhlenbeck Process.** For Ornstein–Uhlenbeck process, $J(t)$ is obtained as:

$$523 \quad J(t) = 2D(1 - e^{-\gamma t})^2 \quad [\text{S-124}]$$

524 In the Ornstein–Uhlenbeck process, a drift acts on the particles. At $t = 0$, when the velocity of the particles is at maximum,
 525 the drift force is also maximized. $J(t)$ starts at 0, and particles have a uniform bulk movement with v_o . As time evolves, the
 526 velocity of the particles and the effect of drift gradually decreases. As the results show, $J(t)$ gradually increases. Eventually,
 527 the system reaches equilibrium and the drift effect is minimized after a long time. In this case, $J(t)$ reaches a plateau at $2D$,
 528 indicating that the system is at equilibrium just like the result from the Wiener process.

$$529 \quad J_{eq}(t) = \lim_{t \rightarrow \infty} 2D(1 - e^{-\gamma t})^2 = 2D \quad [\text{S-125}]$$

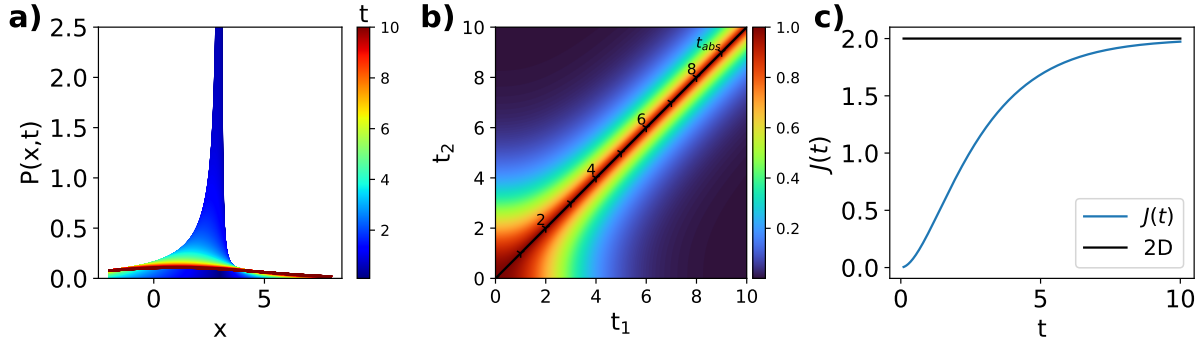


Fig. S2. Simulation for Ornstein–Uhlenbeck Process with $D = 1$, $\gamma = 0.5$, $v_o = -1$ and $x_0 = 3$. The dynamical transport coefficient $J(t) = 2D(1 - e^{-\gamma t})^2$.

530 **B.3. Brownian Oscillator.** For Brownian oscillator, $J(t)$ is obtained as:

$$531 \quad J(t) = \frac{2D\gamma^2}{\omega_s^2} e^{-\gamma t} \sin(\omega_s t)^2 \quad [\text{S-126}]$$

532 Recall that ω_s is a reduced frequency defined in Equation S-120 as $\omega_s = (\omega_o^2 - \frac{1}{4}\gamma^2)^{\frac{1}{2}}$. In the case of underdamping
 533 oscillator as $\omega_o > \frac{1}{2}\gamma$, ω_s is a real and positive value.

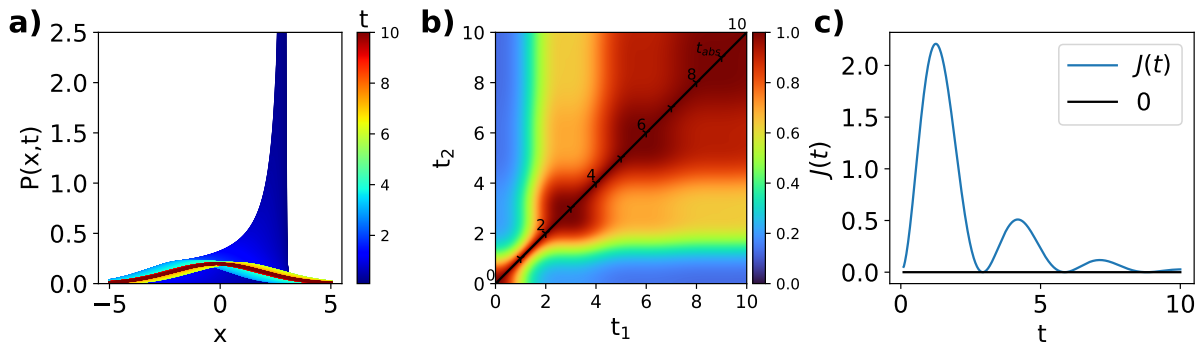


Fig. S3. Simulation for underdamped Brownian Oscillator with $D = 10$, $\gamma = 0.5$, $\omega_o = 1.1$, $v_o = 1$ and $x_0 = 3$.

534 However, in the case of an overdamped oscillator with $\omega_o < \frac{1}{2}\gamma$, ω_s is an imaginary number, and the trend of equation
 535 S-126 is less obvious. Instead, we define a new simplified term of "simplified drift" as $\gamma_s = (\gamma^2 - 4\omega_o^2)^{\frac{1}{2}}$. The term is a real
 536 and positive number when $\omega_o < \frac{1}{2}\gamma$ and consists of relations with ω_s as $\gamma_s = i2\omega_s$. Substituting γ_s into equation S-126 and
 537 applying a relation $\sin(ix) = i \sinh(x)$, we have an equivalent equation for an overdamped oscillator:

$$538 \quad J(t) = \frac{8D\gamma^2}{\gamma_s^2} e^{-\gamma t} \sinh\left(\frac{1}{2}\gamma_s t\right)^2 \quad [\text{S-127}]$$

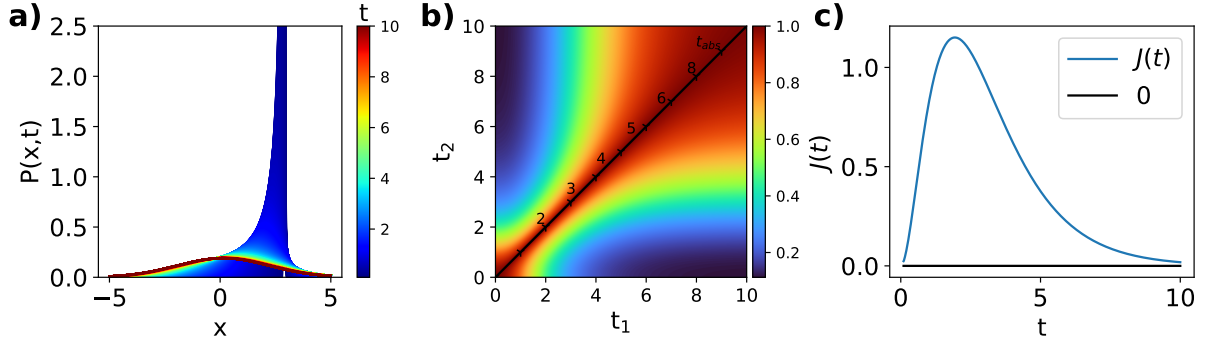


Fig. S4. Simulation for overdamped Brownian Oscillator with $D = 1$, $\gamma = 1.1$, $\omega_o = 0.5$, $v_o = 1$ and $x_0 = 3$.

539 With eq. (S-126) and eq. (S-127), the dynamics of the Brownian oscillator are obvious. For $t \rightarrow \infty$, the term of $e^{-\gamma t}$
 540 dominates $J(t)$ and $J(t) = 0$. This means that the drift force and elastic force cancel out at equilibrium and the system remains
 541 static. For $t \rightarrow 0$, the oscillation term $(\sin(\omega_s t)^2)$ in eq. (S-126) or $(\sinh(\frac{1}{2}\gamma_s t)^2)$ in eq. (S-127) dominates $J(t)$. However,
 542 $J(t)$ as shown in fig. S3 and S4, the oscillation signals vanish much faster for $\sinh^2 \frac{1}{2}\gamma_s t$, as the drift force prevails in the
 543 overdamped oscillator.

544 To reduce the Brownian oscillator to the Ornstein-Uhlenbeck process, we have no external force in the system as

$$545 \begin{aligned} F_{ex} &= m\omega_o^2 x = \omega_o = 0 \\ \gamma_s &= (\gamma^2 - 4\omega_o^2)^{\frac{1}{2}} = \gamma \end{aligned} \quad [S-128]$$

546 Substituting $\gamma_s = \gamma$, the expression of $J(t)$ can be written as:

$$547 \begin{aligned} J(t) &= \frac{8D\gamma^2}{\gamma^2} e^{-\gamma t} \sinh\left(\frac{1}{2}\gamma t\right)^2 \\ &= 8De^{-\gamma t} \left(\frac{1 - e^{-\gamma t}}{2e^{-\frac{1}{2}\gamma t}}\right)^2 \\ &= 2D(1 - e^{-\gamma t})^2 \end{aligned} \quad [S-129]$$

548 By setting ω_0 to 0, we simplify the dynamics from a Brownian Oscillator to an Ornstein-Uhlenbeck process. Additionally, if
 549 the system reaches equilibrium as t tends to infinity as in equation (S-125), the dynamical process further simplifies from an
 550 Ornstein-Uhlenbeck process to a Wiener process, which is the most fundamental stochastic dynamics process.

551 **C. Molecular Dynamics Simulation.** To verify the proposed model, we simulate a solution of non-interacting particles (phantom
 552 particles) in a non-equilibrium system. The solvent is implicitly modeled by the Langevin thermostat, and the equation of
 553 motion of the n -th particle is,

$$554 \vec{v}_n = -\gamma \vec{v}_n + \frac{\vec{\eta}_n(t)}{m} \quad [S-130]$$

555 where the mass, m , is set to unity for all particles, $\vec{v}_n(t)$ is the velocity of the n -th particle. The stochastic force acting on the
 556 n -th particle, $\vec{\eta}_n(t)$, satisfies the following conditions,

$$557 \begin{aligned} \mathbb{E}[\vec{\eta}_n(t)] &= \vec{0} \\ \mathbb{E}[\vec{\eta}_n(t) \otimes \vec{\eta}_n(t')]_{ij} &= 6k_B T \gamma \delta_{ij} \delta(t - t') \end{aligned} \quad [S-131]$$

558 The friction coefficient, γ , is set to $\gamma = 1000 \frac{m}{\tau}$, where $\tau = \sigma \left(\frac{m}{\epsilon}\right)^{\frac{1}{2}}$ is the reduced time, σ and ϵ are reduced length and
 559 energy, respectively. The velocity-Verlet algorithm is used to integrate the equation of motion, with an integration time step
 560 $\Delta t = 0.001\tau$. The simulation consists of three stages with different temperatures:

- 561 1. The temperature was kept constant at $T = 5 \frac{\epsilon}{k_B}$.
- 562 2. The temperature linear decreased with time from $T = 5 \frac{\epsilon}{k_B}$ to $T = 0.1 \frac{\epsilon}{k_B}$.
- 563 3. The temperature was maintained constant at $T = 0.1 \frac{\epsilon}{k_B}$.

564 Each stage lasts for 1τ , that is, 1000 simulation steps. All simulations were performed using the Large Scale Atomic /
 565 Molecular Massively Parallel Simulator (LAMMPS) (6) under periodic boundary conditions.

566 In the paper, c_2 and its corresponding analysis for bins at $q_x = 6$, $q_y = q_x = 6$ and $q_x = q_y = q_z = 6$ have been demonstrated.
 567 Here, we provide the bins at $q_x = 3$, $q_y = q_x = 3$ and $q_x = q_y = q_z = 3$ to further verify the non-equilibrium analysis approach.
 568 Again, $J(t)$ obtained from two respective approaches, derived from analyzing c_2 of XPCS and spatial averaging of the particle
 569 positions in the simulation box, shows consistency. This result provides evidence that $J(t)$ accurately reflects the actual physical
 570 quantity in the system, validating the extraction approach of $J(t)$.

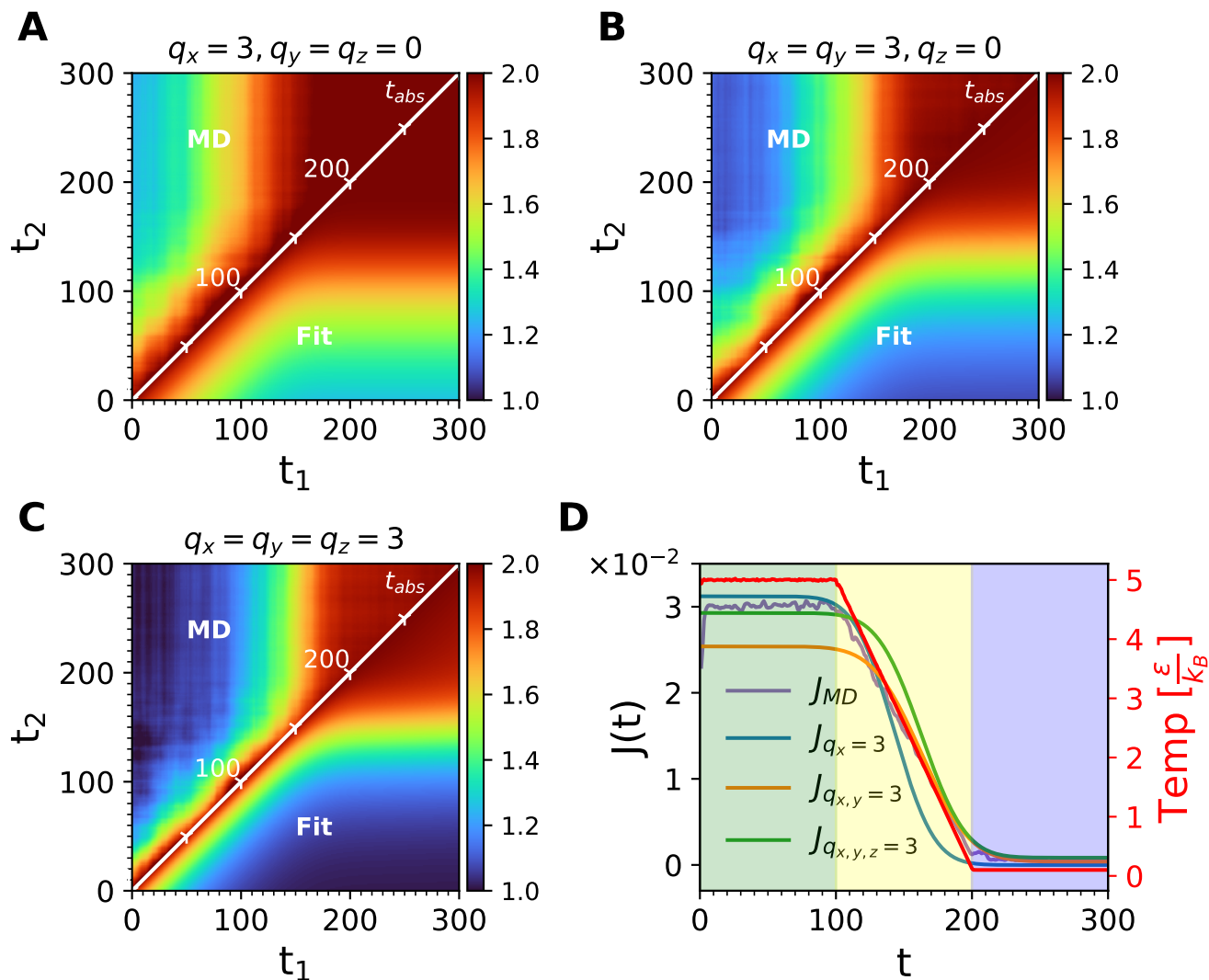


Fig. S5. Application of the model analysis on a simulated non-equilibrium system reveals three distinct stages of temperature change, which are visually represented by the filled-in background color.

571 5. Correlating Microscopic Dynamics with Macroscopic Rheology through $J(t)$ in Rheo-XPCS

572 **A. Supplementary Results: Recovery following a 10 Pa Creep Test.** Beyond the relaxation data for the 10 Pa creep test
 573 illustrated in Figures 3A and 3C of the primary manuscript, we further examined the XPCS data derived from a 10 Pa creep
 574 test, as detailed in Figure 2A as reference (7). The aggregated findings of the 10 Pa and 100 Pa creep tests are presented in
 575 Figure Fig. S6 in this document.

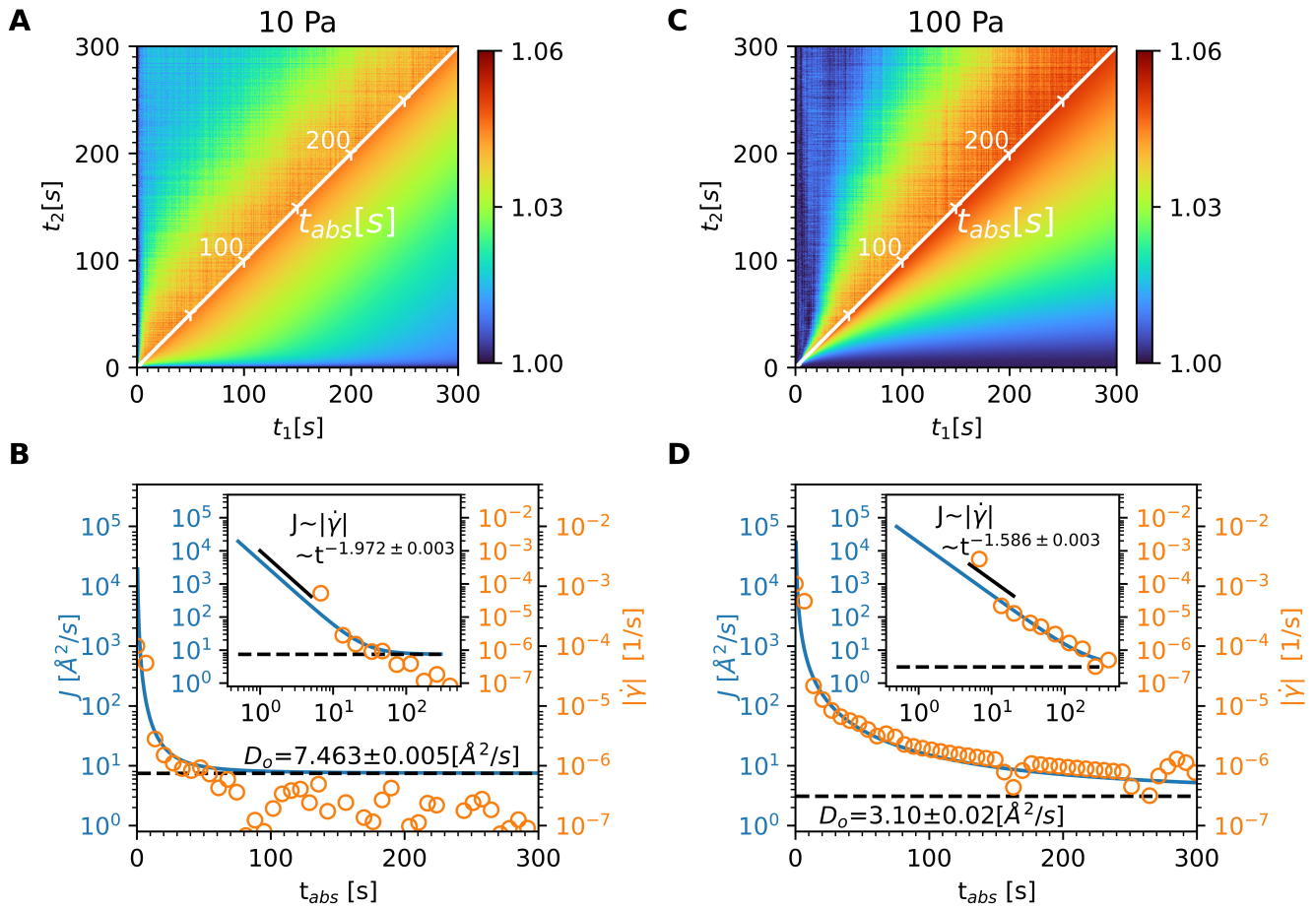


Fig. S6. Comparative Analysis of the $J(t)$ and the shear ($\dot{\gamma}(t)$) During the Recovery Phase of Creep Tests. Panels A and B illustrate the relationship between $J(t)$ and $\dot{\gamma}(t)$ under an applied stress ($\sigma(t)$) of 10 Pa, while Panels C and D show the same under a $\sigma(t)$ of 100 Pa (also shown in Fig 3 A and B in the main texts). From Panels B and D, a consistent scaling relation of $\frac{k_B T}{\pi r}$ is observed between $J(t)$ and $\dot{\gamma}(t)$, independent from the applied $\sigma(t)$ in the creep test.

576 Analysis of Fig. S6 yields several key insights:

- 577 1. During the creep tests, the $J(t)$ diminishes more swiftly at the lower stress level (10 Pa) with an exponent of -1.972 , in
 578 contrast to the -1.586 exponent observed under the higher stress condition (100 Pa). This trend aligns with the results
 579 of both XPCS, evidenced by a pronounced increase in c_2 along the t_{abs} diagonal, and rheological data, which show $\dot{\gamma}(t)$
 580 approaching zero as the strain quickly returns to the baseline level of irrecoverable strain.
- 581 2. The estimated values of D_o from both creep tests are similar in magnitude. However, the lack of extended c_2 data for the
 582 100 Pa creep test compromises the precision of D_o , leading to the observed variance in the values D_o between panels B
 583 and D.
- 584 3. The rapid recovery observed in the 10 Pa creep test results in a rapid decrease in $\dot{\gamma}(t)$, potentially falling below the
 585 sensitivity range of the measurement instruments, thus casting doubt on the reliability of the data points with $\dot{\gamma} < 10^{-6}$.
 586 Despite this, Fig. S6 generally demonstrates a consistent scaling relation between $J(t)$ and $\dot{\gamma}(t)$.

587 In the following section, we will concentrate on the third conclusion to further explore the intrinsic relationship between the
 588 $J(t)$ and $\dot{\gamma}(t)$.

589 **B. $J(t)$ and $\dot{\gamma}(t)$ in micro-rheology.** To elucidate this phenomenon, we used Equation (9) to correlate the variance in position
 590 ($\mathbb{V}[x(t)]$) and creep compliance ($\mathcal{J}(t)$) from reference (8), which is presented as follows:

591
$$\mathbb{V}[x(t)] = \frac{k_B T}{\pi r} \mathcal{J}(t) = \frac{k_B T}{\pi r \sigma} \dot{\gamma}(t) \quad [\text{S-132}]$$

592 where r represents the radius of the particles involved. By differentiating both sides for time, we derive an expression that links
 593 $J(t)$ and $\dot{\gamma}(t)$ through a scaling factor of $\frac{k_B T}{\pi r \sigma}$,

$$J(t) = \frac{k_B T}{\pi r \sigma} \dot{\gamma}(t) \quad [\text{S-133}]$$

However, the scaling between $J(t)$ and $\dot{\gamma}(t)$ obtained from reference (7) and as shown in Fig. S6 of our manuscript does not align with eq. (S-133). As indicated in reference (8), the theoretical derivations in micro-rheology suggest a scaling factor of $\frac{k_B T}{\pi r \sigma}$, indicating discrepancies attributable to the recovery-phase measurements of viscoelastic materials, which deviate from the assumed creeping flow conditions.

Interestingly, through our analysis, we observed a power-law decrease of $J(t)$ correlates with the rheometric shear rate via a scaling factor $\frac{k_B T}{\pi r}$, assuming $r = 10\text{nm}$ and $T = 298\text{K}$, as specified in the experiments from reference (7). Ignoring the units for a moment, this leads us to an empirical formulation:

$$J(t) \approx \frac{k_B T}{\pi r} |\dot{\gamma}(t)| \quad [\text{S-134}]$$

This empirical relation, although not theoretically derived, offers a pragmatic approximation under the specific conditions of our experiments. Fig. S7 is corroborated by the results of the creep test performed under a lower stress of 10 Pa, indicating that the observed scaling between $J(t)$ and $\dot{\gamma}(t)$ is not affected by the magnitude of the applied creep stress.

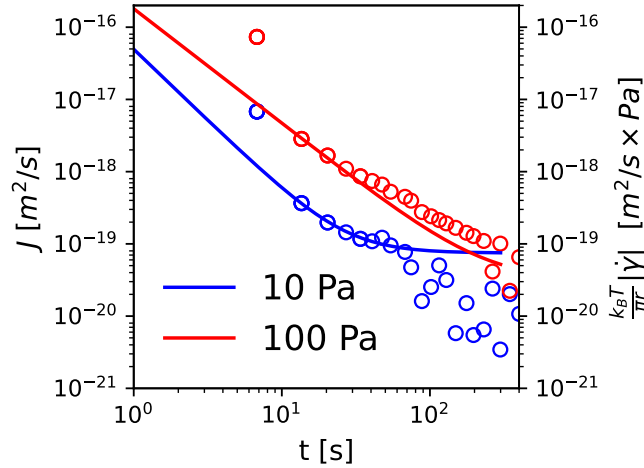


Fig. S7. The connection between microscopic dynamics ($J(t)$) and macroscopic properties ($\dot{\gamma}(t)$) in the recovery phase of creep tests with $\sigma(t)$ of 10Pa (blue) and 100Pa (red). The $J(t)$ (solid line) is derived from non-equilibrium analysis on c_2 measured by XPCS, and the $\dot{\gamma}(t)$ obtained from the rheometer, then scaled by a factor of $\frac{k_B T}{\pi r}$ (scattered dots), is measured from rheometer. For a better comparison, the unit for both $J(t)$ and $\dot{\gamma}(t)$ have been converted to International System of Units (S.I. Units)

Our ongoing research is focused on elucidating these findings and developing a theoretical framework to accurately describe them. In simulations involving phantom particles, we observed that the variations in $J(t)$ and $\dot{\gamma}(t)$ over time are decoupled; the shear rate induces affine transformations that alter the central positioning of the intensity profile $\text{IP}(x, t)$ without affecting the distribution breadth and, consequently, $J(t)$. A preliminary hypothesis suggests that external deformation in such systems, characterized by complex potentials, can induce systematic forces, including frictional and interparticle forces, thereby influencing transport dynamics. We are actively working to further explore and define these dynamics and to develop a comprehensive theoretical model. Our goal is to bridge microscopic $J(t)$, as determined by XPCS, with macroscopic rheological properties, such as the complex shear modulus ($G^*(\omega)$) and the stress relaxation modulus ($G_r(t)$), using the principles of microrheology discussed in (9).

6. Microscopically Heterogeneous Dynamics

In reference (7), the microscopically heterogeneous dynamics is quantified using the ratio of the recovery to quiescence phases in c_2 , denoted as $c_{\text{ratio}}(t_1, t_2 = 0)$ in equation [3] from their paper.

Our methodology introduces an alternative approach for assessing the microscopically heterogeneous dynamics. As delineated in the derivations eqs. (S-4) and (S-5), our model assumes random, homogeneous, and independent particle dynamics. This assumption leads to the simplification where terms involving $n \neq m$ average to zero, yielding our non-equilibrium model. Given this foundation, the correlations we analyzed pertain mainly to diffusive and nonaffine dynamics, denoted $c_{2,\text{Homo}}$, and do not directly correspond to the microscopically heterogeneous dynamics described in the paper (7).

However, our current work has devised a method to discern such complex dynamics. To elucidate the contributions from heterogeneous dynamics ($c_{2,\text{Hetero}}$), we employ the following expression:

$$c_{2,\text{Hetero}} \sim \mathbb{E} \left[\sum_{n=1}^N \sum_{m \neq n}^N e^{i\vec{q} \cdot (\vec{r}_n(t_2) - \vec{r}_m(t_1))} \right] = c_{2,\text{exp}} - c_{2,\text{Homo}} \quad [\text{S-135}]$$

626 This approach involves subtracting the component of homogeneous dynamics from the total experimental correlation, thus
627 isolating the residuals that reflect heterogeneous dynamics, as demonstrated in Fig. S8.

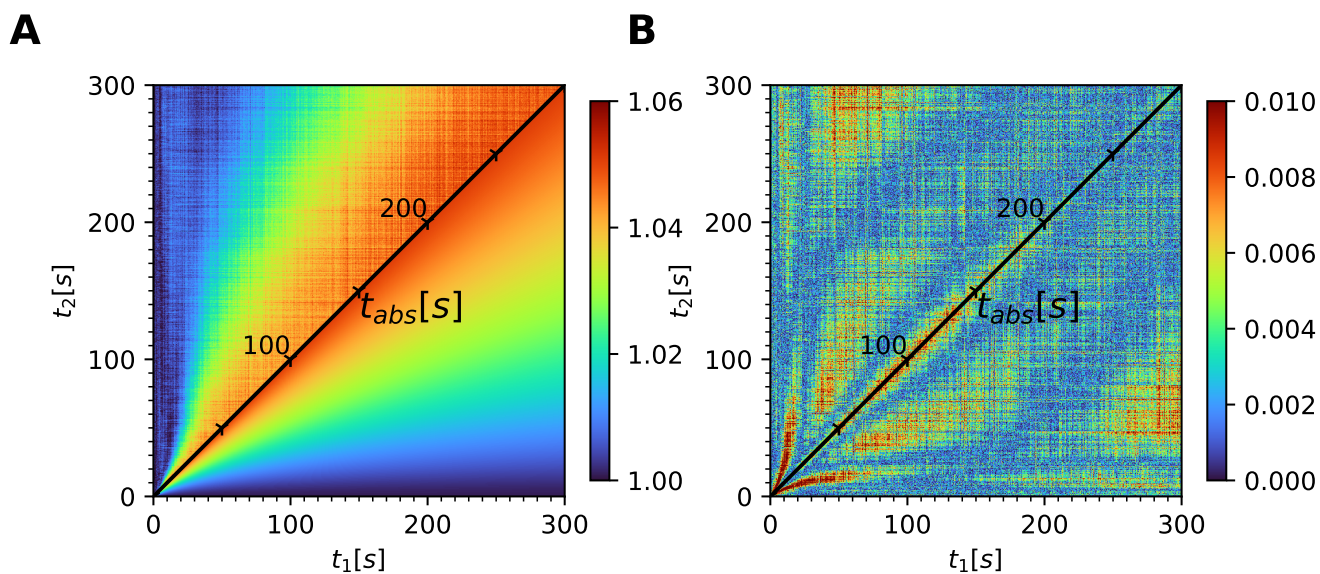


Fig. S8. Illustrating microscopically heterogeneous dynamics during recovery: By subtracting the diffusive dynamics attributed to c_2 based on the non-equilibrium model (Panel. A, lower right) from experimental c_2 measurements (Panel. A, upper left), the c_2 serves as evidence of microscopically heterogeneous dynamics in Panel B, indicating interference between at least two compositions with distinct dynamics in the system. The 'tailing' shape of the c_2 is largely attributed to the abrupt halt of a thin flow layer near the rotor during the recovery phase, mirroring the microscopically heterogeneous changes detailed in reference (7).

628 The temporal patterns observed in the residuals of c_2 shown in Fig. S8 suggest the presence of microscopically heterogeneous
629 dynamics, as previously noted by (7). The pronounced 'tailing' pattern evident in S8B is indicative of shear banding, potentially
630 resulting from the sudden stop of a thin flow layer near the rotor's surface during the recovery phase. This aligns with
631 the heterogeneous dynamics discussed in (7). We are currently enhancing our methods to more effectively formalize these
632 relationships, accurately describe the patterns seen in c_2 , and quantify the associated heterogeneous dynamics.

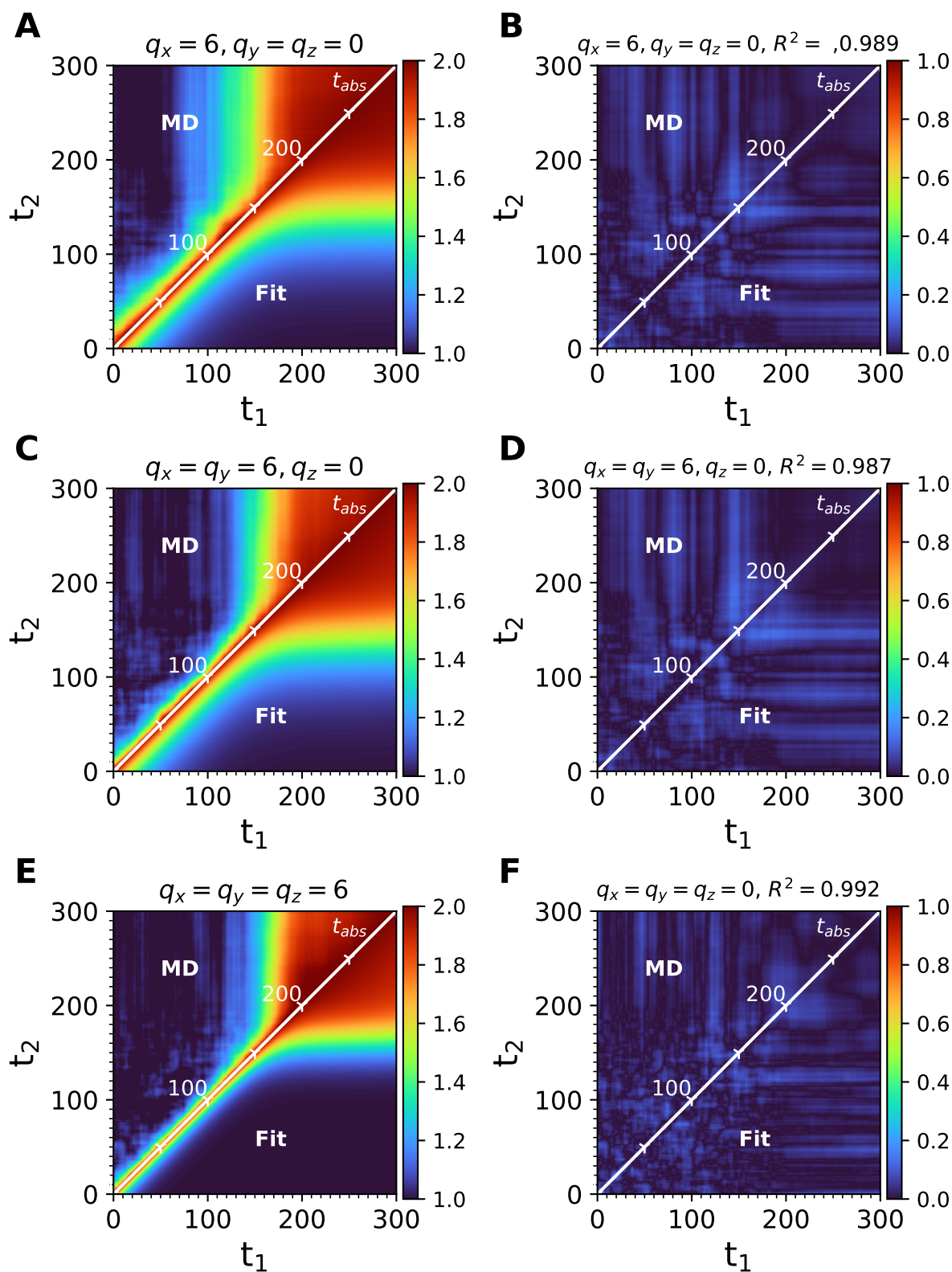


Fig. S9. illustration of the fitting results (Panels A, C, E) and residuals (Panels B, D, F) obtained after the data fitting process shown in Fig. 2 of the main manuscript. The R^2 of the fitting is shown in the title of the residual plot.

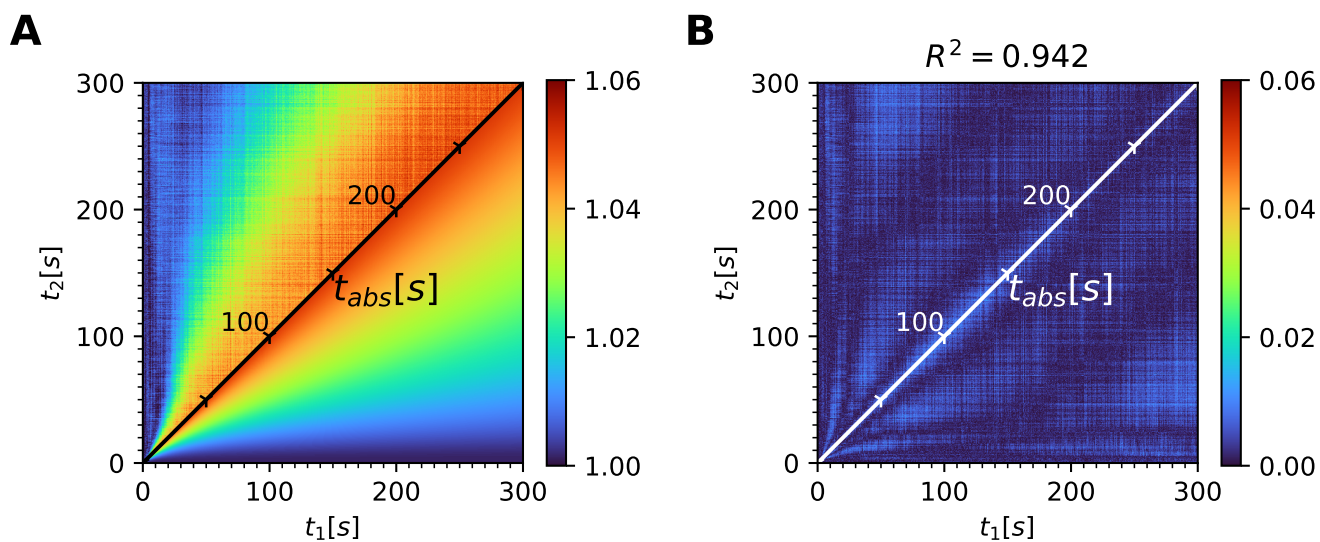


Fig. S10. Illustration of the fitting results (Panel. A) and residuals (Panel. B) obtained after the data from the (7) fitting process shown in Fig. 3A of the main manuscript. The R^2 of the fitting is shown in the title of the residual plot.

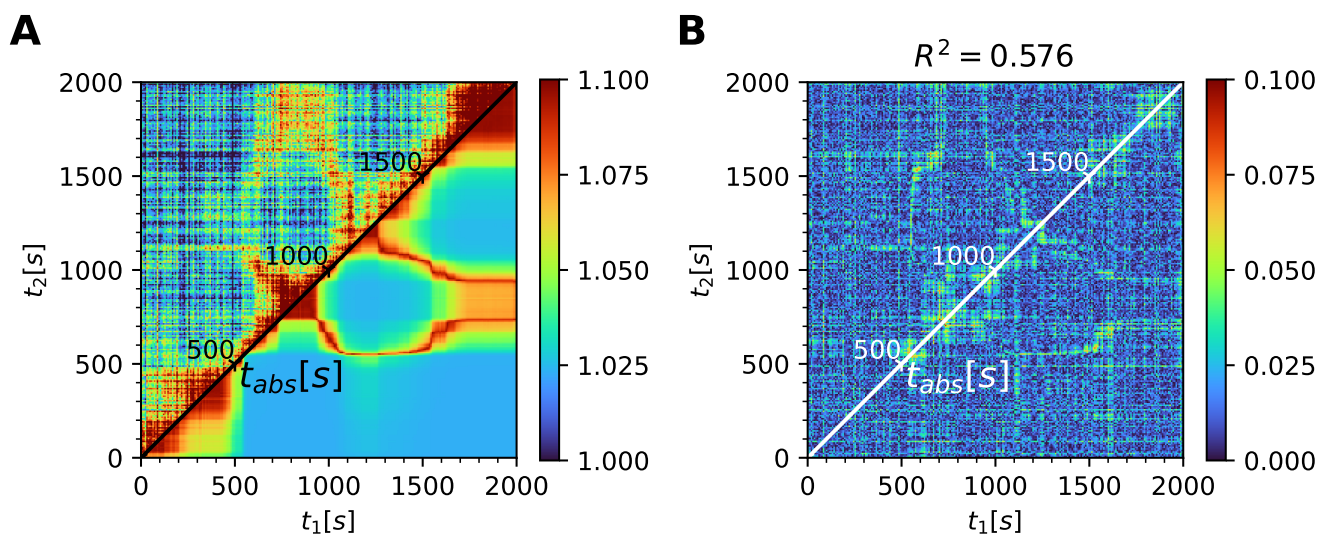


Fig. S11. Illustration of fitting results (Panel. A) and residuals (Panel. B) obtained after the data from (10) fitting process shown in Fig. 3C of the main manuscript. The R^2 of the fitting is shown in the title of the residual plot.

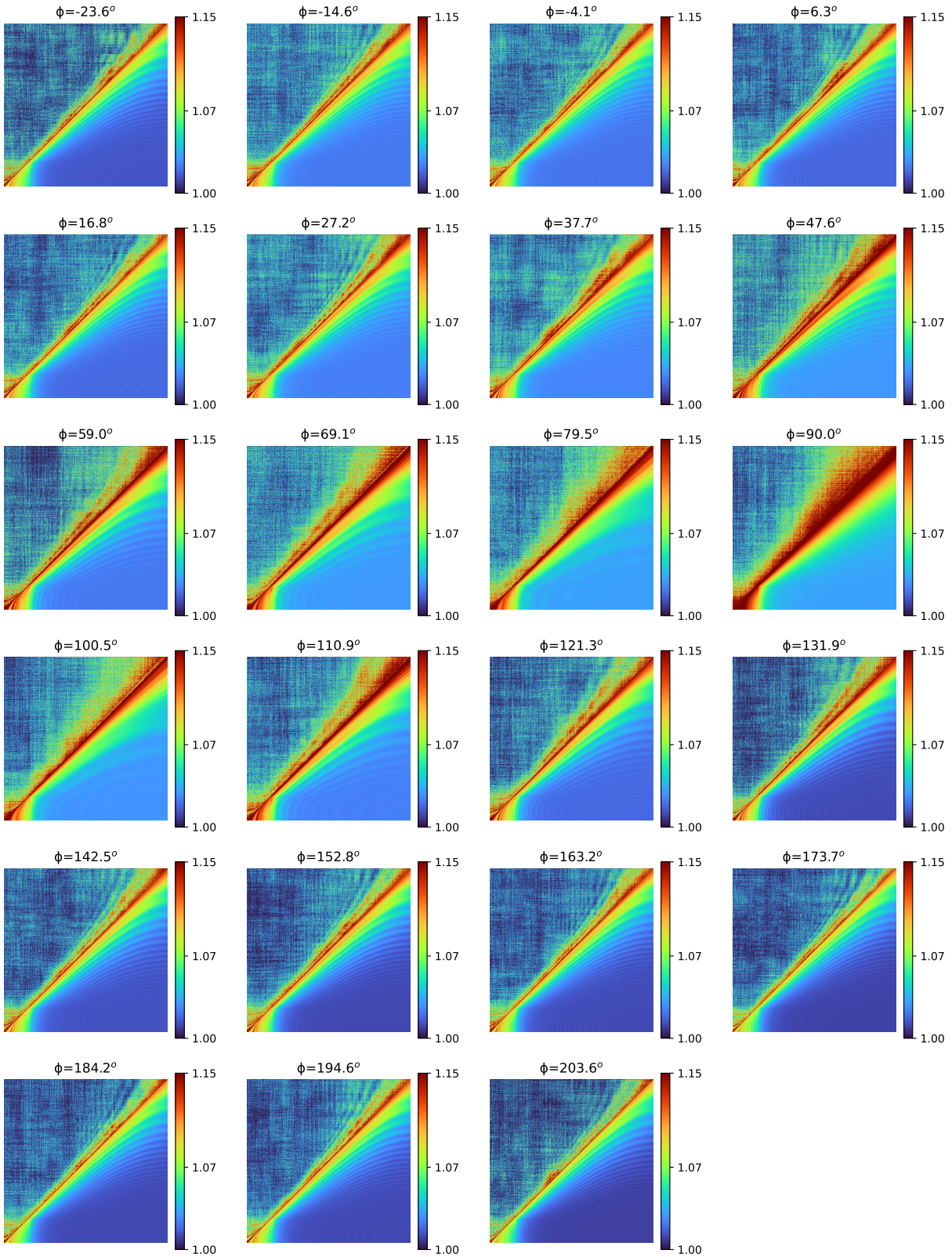


Fig. S12. Comprehensive c_2 data across all ϕ directions from Fig. 4 of the manuscript. The angle ϕ , corresponding to each bin on the field detector, is marked in the title of each panel for reference. One shown in Fig 4 of the main text is at $\phi = 6.3^\circ$.

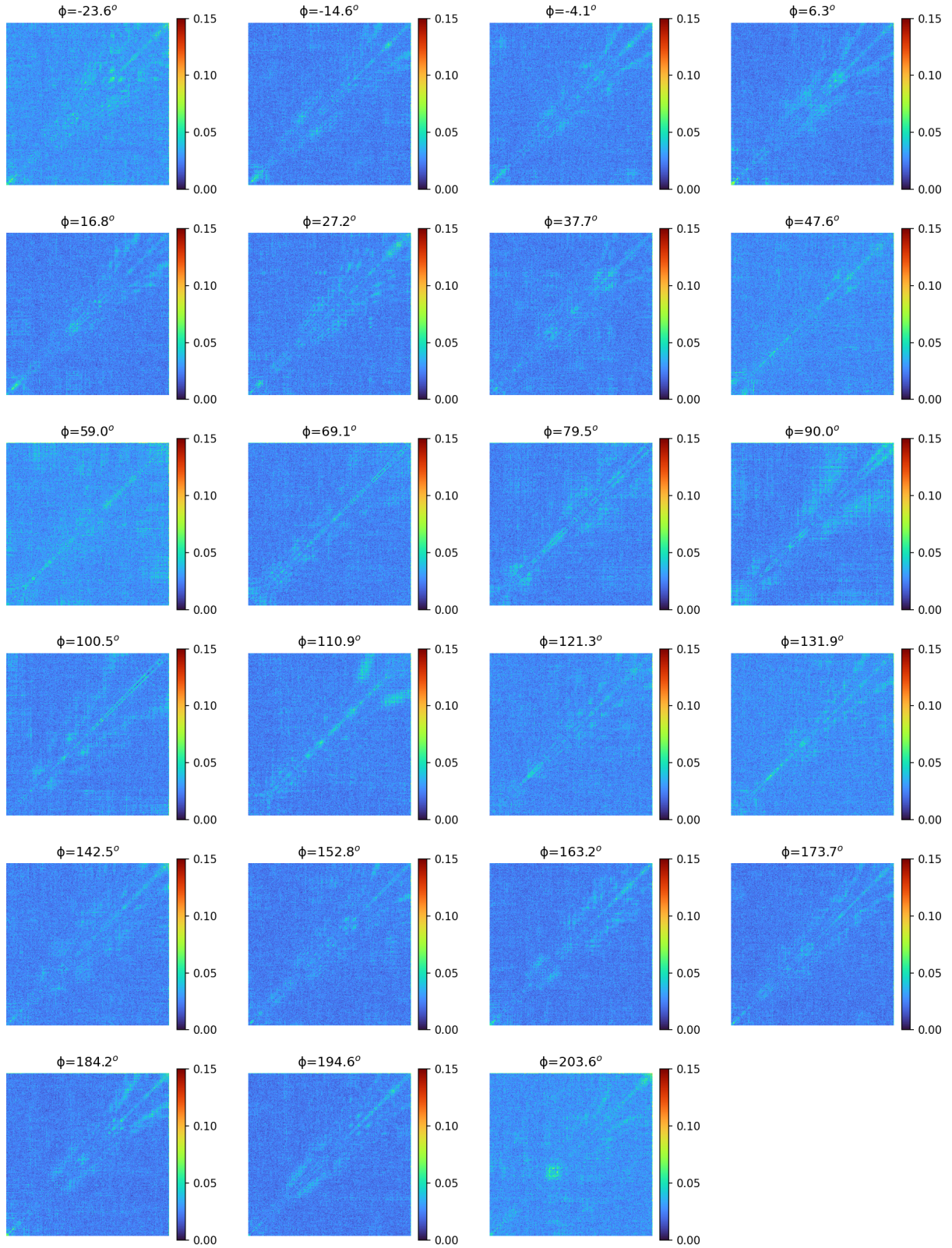


Fig. S13. Presentation of the residuals resulting from the analysis conducted in Fig. 4 of the manuscript, encompassing all ϕ directions. The angle ϕ , corresponding to each bin on the field detector, is marked in the title of each panel for reference.

637 **References**

- 638 1. J Lhermitte, Using Coherent X Rays to Measure Velocity Profiles. (McGill University (Canada)), (2015).
639 2. R Loudon, The quantum theory of light. (OUP Oxford), (2000).
640 3. V Balakrishnan, Elements of nonequilibrium statistical mechanics. (Springer) Vol. 3, (2008).
641 4. G Röpke, Nonequilibrium statistical physics. (John Wiley & Sons), (2013).
642 5. S Chandrasekhar, Stochastic problems in physics and astronomy. Rev. modern physics **15**, 1 (1943).
643 6. S Plimpton, Fast parallel algorithms for short-range molecular dynamics. J. computational physics **117**, 1–19 (1995).
644 7. GJ Donley, et al., Investigation of the yielding transition in concentrated colloidal systems via rheo-xpcs.
645 Proc. Natl. Acad. Sci. **120**, e2215517120 (2023).
646 8. J Xu, V Viasnoff, D Wirtz, Compliance of actin filament networks measured by particle-tracking microrheology and
647 diffusing wave spectroscopy. Rheol. acta **37**, 387–398 (1998).
648 9. TG Mason, DA Weitz, Optical measurements of frequency-dependent linear viscoelastic moduli of complex fluids.
649 Phys. review letters **74**, 1250 (1995).
650 10. J Song, et al., Microscopic dynamics underlying the stress relaxation of arrested soft materials. Proc. Natl. Acad. Sci.
651 **119**, e2201566119 (2022).